LIGHTHOUSE REPORTS

Safe and Sustainable Sea Transport Through Development of Test Method for Foiling Craft

An innovation project conducted within the Swedish Transport Administration’s industry programme for Sustainable Shipping, led by Lighthouse and published in August 2026.

www.lighthouse.nu

Safe and Sustainable Sea Transport Through Development of Test Method for Foiling Craft

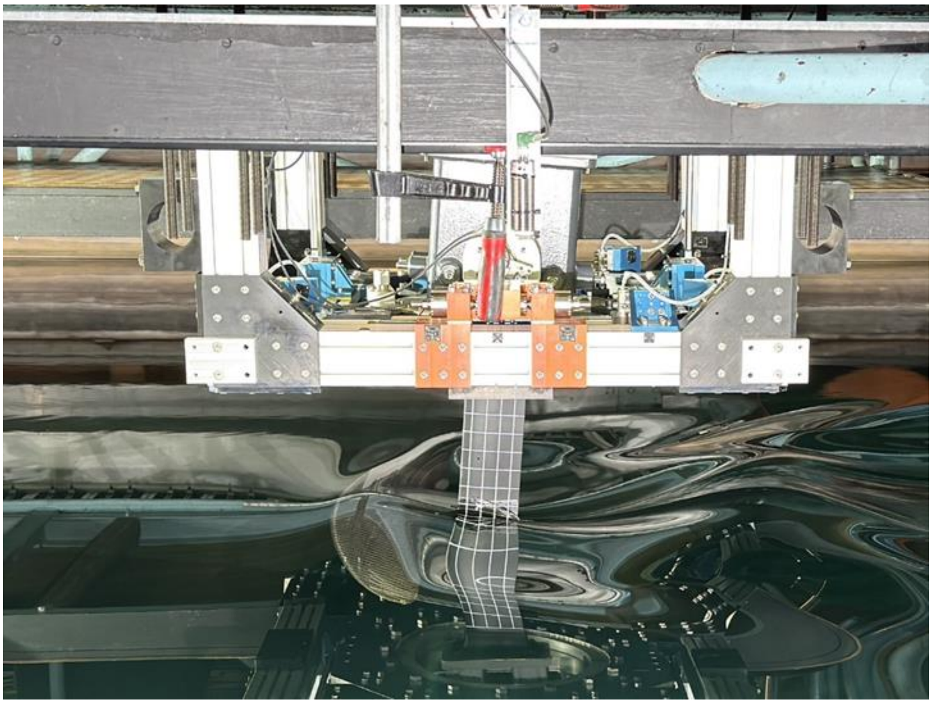

Authors

Alex Shiri, RISE

Arash Eslamdoost, Chalmers University of Technology

In Collaboration with

KTH, SSRS, Aston Harald

An innovation project carried out within the Swedish Transport Administration's industry program Sustainable Shipping, operated by Lighthouse

Summary

The growing demand for sustainable and energy efficient marine transportation, driven by advances in electric propulsion and increasing environmental concerns, has led to renewed interest in hydrofoil technology. By lifting the hull out of the water during transit, hydrofoils can dramatically reduce hydrodynamic resistance, enabling higher efficiency, extended operational range, reduced noise emissions, and improved passenger comfort. These characteristics make foiling craft particularly attractive for electric ferries, high speed service vessels and autonomous craft.

Despite their significant potential, the hydrodynamics and dynamic behaviour of foiling craft remain insufficiently understood. Hydrofoils operate in a highly dynamic and complex environment involving strong interactions between the foil, free surface, hull, and waves. Key challenges include accurate prediction of lift and drag across relevant operating conditions, foil behaviour in waves, foil ventilation, operation close to free-surface and near failure scenarios such as sudden descents. Furthermore, unlike displacement vessels, hydrofoil performance depends strongly on both submergence and Reynolds number, making conventional Froude based scaling procedures inadequate. The lack of established testing guidelines and scaling methodologies has limited the effectiveness and reliability of experimental investigations.

Previous experimental studies at the RISE Maritime/SSPA facilities have examined hydrofoil performance through towing tank measurements, cavitation tunnel investigations of fluid-structure interaction, and foiling model boat tests conducted within academic and applied research projects. However, because existing towing tank configurations are optimized for conventional hull testing, these studies required improvised mounting solutions and test rigs. This increased cost, complexity and, in some cases, compromised measurement accuracy due to structural compliance, limited measurement capability, and insufficient control of foil position and angle of attack.

To address these challenges, the present project focuses on the development of tailored experimental methods and dedicated measurement rig for hydrofoil testing. A new test rig has been designed and manufactured to enable accurate measurement of all relevant force and moment components while allowing precise control and monitoring of foil submergence, motion, and angle of attack. Full scale hydrofoils are tested to reduce Reynolds number scaling uncertainties, and a systematic test matrix is conducted in the RISE Maritime/SSPA towing tank using multiple foil sizes, submergence conditions, and operating conditions. Both calm water condition and response to regular waves in head and following seas are investigated. The results are presented together with an assessment of dominant contributors to measurement uncertainties.

The objective of this work is to establish reliable experimental methodologies for hydrofoil performance assessment in controlled and dynamic conditions, improve measurement practices of hydrofoils, and enhance understanding of hydrofoil behaviour relevant to design, safety, and efficiency. The knowledge generated is intended to support designers, operators, and test facilities in advancing high performance, low emission foiling craft. The project is carried out as a close collaboration between the RISE Maritime Department and Chalmers University of Technology.

Sammanfattning

Den växande efterfrågan på hållbar och energieffektiva lösningar för marin transport, i kombination med tekniska framsteg inom elektrisk framdrivning och ökad krav på minskad miljöpåverkan, har bidragit till ett återuppväckt intresse för andvändningen av hydrofoilteknik inom sjöfartssektorn. Genom att lyfta skrovet ur vattnet under gång kan hydrofoiler kraftigt minska det hydrodynamiska motståndet, vilket möjliggör högre verkningsgrad, utökad operativ räckvidd, reducerade buller och förbättrad passagerarkomfort. Dessa egenskaper gör foilande farkoster särskilt attraktiva för elektriska färjor, höghastighetsfartyg i service och autonoma farkoster.

Trots deras stora potential är hydrodynamiken och det dynamiska beteendet hos foilande farkoster fortfarande otillräckligt förstådda. Hydrofoiler verkar i en dynamisk och komplex miljö med kraftiga interaktioner mellan foilen, den friytan, skrovet och vågor. Centrala utmaningar inkluderar noggrann förutsägelse av lyftkraft och motstånd under relevanta driftförhållanden, foilbeteende i vågor, foilventilation, drift nära friytan samt nära haveriscenarier såsom plötslig nedsjunkning. Vidare skiljer sig hydrofoilers prestanda från deplacementfartyg genom ett starkt beroende av både nedsänkningsdjup och Reynolds tal, vilket gör konventionella Froude baserade skalningsmetoder otillräckliga. Avsaknaden av etablerade provningsriktlinjer och skalningsmetoder har begränsat effektiviteten och tillförlitligheten hos experimentella studier.

Tidigare experimentella studier vid RISE Maritime/SSPA:s anläggningar har undersökt hydrofoilprestanda genom mätningar i provningsränna, undersökningar av FSI i kavitationstunnel samt provningar av foilande modellbåtar inom ramen för akademiska och tillämpade forskningsprojekt. Eftersom befintliga dragtankkonfigurationer är optimerade för konventionell skrovprovning krävde dessa studier improviserade uppmonteringslösningar och provriggar. Detta ökade kostnader och komplexitet och i vissa fall försämrat mätnoggrannheten till följd av strukturell följsamhet, begränsad mätkapacitet samt otillräcklig kontroll av foilens position och vinkel.

För att hantera dessa utmaningar fokuserar det aktuella projektet på utveckling av anpassade experimentella metoder och en dedikerad mätrigg för hydrofoilprovning. En ny provrigg har konstruerats och tillverkats för att möjliggöra noggrann mätning av samtliga relevanta kraft- och momentkomponenter, samtidigt som exakt kontroll av foilens nedsänkningsdjup, rörelse och anfallsvinkel tillåts. Fullskaliga hydrofoiler provas för att reducera osäkerheter kopplade till Reynoldstals skalning, och en systematisk testmatris genomförs i RISE Maritime/SSPA:s provningsränna med användning av flera foilstorlekar, nedsänkningsnivåer och driftförhållanden. Både lugnvattenförhållanden och foilens respons på regelbundna vågor i mötande och medgående riktning undersöks. Resultaten presenteras tillsammans med en analys av de dominerande bidragen till mätosäkerheterna.

Syftet med detta arbete är att etablera tillförlitliga experimentella metoder för utvärdering av hydrofoilprestanda under kontrollerade och dynamiska förhållanden, förbättra mätpraxis för hydrofoiler samt fördjupa förståelsen av hydrofoilbeteende med relevans för design, säkerhet och effektivitet. Den genererade kunskapen är avsedd att stödja konstruktörer, operatörer och provningsanläggningar i utvecklingen av högpresterande, lågutsläppande foilande farkoster. Projektet genomförs i nära samarbete mellan RISE Maritims avdelning och Chalmers tekniska högskola.

Contents

1 Introduction

The concept of hydrofoils (foiling craft) has existed for nearly a century. In parallel with the development of aerodynamic airfoils and their adoption in aviation, early marine researchers recognized that lifting surfaces could also be used to reduce hydrodynamic resistance in waterborne vehicles [1]. Over time, numerous foiling crafts have been designed and built with varying degrees of commercial and operational success (Figure 1).

Figure 1- Curl II, hydrofoil ferry in operation in Sydney Harbor from 1973 to 1992. (www.bairdmaritime.com)

Historically, the primary motivation for adopting hydrofoils was to achieve higher vessel speed. Consequently, many early designs targeted power boats and high-speed passenger ferries. However, advances in conventional propulsion and hull forms, particularly high-power engines and waterjet propulsion enabled very high cruise speeds even for planning craft. Given the operational complexity of early foiling systems, the relative advantage of hydrofoils as a high-speed solution diminished in many applications.

In recent years, foiling has regained significant attention for a different reason: energy efficiency, particularly in the context of electric propulsion. Because batteries have limited energy-to-weight ratios compared with liquid fuels, increasing an electric vessel's range by adding batteries can quickly increase displacement and, in turn, required propulsive power. Foiling offers a pathway to reduce total resistance at higher speeds by transferring a substantial portion of the craft weight from buoyant support to hydrodynamic lift. This reduction in power demand can enable lighter battery packs and longer range for a given energy capacity.

This renewed feasibility is also enabled by technological advancements, including lightweight composite structures, low latency sensors and control systems, and compact submersible electric motors. Together, these developments have made it possible to redesign foiling craft with the objective of minimizing required propulsion power and supporting low or zero emission maritime transportation.

Optimizing foiling craft performance requires understanding not only steady lift and drag, but also dynamic behaviour under realistic operating conditions, such as near surface operation, wave encounter, and controlled changes in foil attitude and submergence. While computational fluid dynamics (CFD) can provide insight, high fidelity simulations of unsteady foil near free surface coupled with dynamic motions remain computationally expensive and sensitive to modelling assumptions.

By contrast, towing-tank experiments provide controlled, repeatable conditions and allow direct measurement of hydrodynamic loads. Importantly, they also offer a practical platform for calibration and validation of sensors and control systems, supporting the development of active foil control systems.

Some advantages of using hydrofoil technologies for vessels are:

- Hydrofoil craft has low resistance and good sea-keeping performance at high speeds, thus allowing the vessel to maintain high speed over time in moderate sea conditions
- Improves the working conditions for the crew.
- Provides stable platform (less slamming in waves).
- Capable of cruising at high speed with efficiency.
- Creates smaller wake and therefore suitable for stealth operation.
- Combined with electric propulsion, it has smaller heat signature.

Despite these advantages, hydrofoil technology also presents several challenges:

- Higher cost of manufacturing
- Complex control system
- Difficult to launch and recovery
- Deeper draft
- Prone to damage in shallow water and ice condition.

1.1 Applications for Hydro-Foiling Vessel

Historically, hydrofoil crafts were limited to a small number of powerful high-speed vessels. Recent technological advances, however, have enabled the development of hydrofoil vessels across a wider range of sizes with significantly lower power requirements. A selection of hydrofoil craft that are currently in production or in operation in the past is presented in the Table 1.

Recent technological advancements contributing to the development of hydrofoil craft include:

- Improved electric motors and battery technologies, which enable longer operational range and reduced system complexity.

- Advanced computerized control systems and sensors, which enhance stability and reduce operational risk.

- The use of lightweight composite materials leads to reduced vessel weight and improved performance.

Table 1 - Examples of hydrofoiling vessels (Candela.com; artemistechnologies.co.uk; mantaraycraft.com and Wikipedia.org).

VESSEL	TYPE	YEAR	ENGINE POWER	CRUISE SPEED	MAX FOILING WEIGHT
CANDELA C-8	powerboat	2022	50 kW - electric	22kt	1.9 tons
MANTARAY M25	powerboat	2024	115 hp – petrol engine	30kt	1.7 tons
METEOR-197	ferry	1960	2000 hp – Diesel	32kt	123 passengers
BOEING 929 JETFOIL	ferry	1976	6MW gas turbine waterjet	45kt	115 tons
CANDELA P-12	ferry	2024	100kW - electric	25kt	10 tons
ARTEMIS EF-24	ferry	-	electric	34kt	150 passengers

ARTEMIS EF-12	Service boat	2026	electric	25kt	11.7 tons
USS PEGASUS	Fast attack Patrol boat	1973	13.4MW gas turbine	48kt	237 tons
SPARVIERO-CLASS	Patrol boat	1973	3.7 MW gas turbine	50kt	60.6 tons
HMCS BRAS D'OR	Anti-submarine	1968	19MW gas turbine	60kt	240 tons
CASPIAN MRK 702	Missile boat	1977	11MW gas turbine	42 kt	257 tons

Power boat:

Foiling powerboats offer high speed and enhanced comfort while requiring relatively low power input. Although foiling technology is particularly well suited to electric propulsion, several vessels also employ conventional combustion engines. Candela and Mantaray are two notable examples of Swedish-designed foiling powerboats.

Candela C-8 ***Mantaray M25***

Passenger Ferries:

Early passenger ferry hydrofoil designs demonstrated the ability to achieve higher operating speeds than conventional ferries. During the 1960s and 1970s, many civil hydrofoil ferries were built in the Soviet Union and the United States, many of which remained in service for several decades. These early designs primarily focused on attaining very high speeds and therefore relied on powerful propulsion systems.

Meteor-197 ***Boing 929 Jetfoil***

In contrast, the current generation of foiling ferries is increasingly being designed for moderate speeds and electric propulsion, resulting in significantly lower power requirements.

Candela P-12

Artemis EF-24

Service Vessels:

There are examples of service vessels and workboats that achieve practical range and high speed by combining electric propulsion with hydrofoiling, such as the Artemis EF-12.

Artemis EF-12

Navy Vessels:

Several types of naval hydrofoil vessels were developed between the 1950s and 1980s, primarily powered by powerful gas turbine engines.

USS Pegasus (PHM-1)

Sparviero-class patrol boat

1.2 Prior work and limitations of existing towing tank setups

RISE Maritime/SSPA has conducted several hydrofoils related experimental studies, including the NACRA17 foil fluid-structure interaction investigations [2], towing tank studies of foiling model boats developed by Chalmers master's students [3] (Figure 2), and work connected to the design a foiling electric craft for the Swedish Sea Rescue Society. Below is a list of relevant projects on foiling in Sweden:

- ELINN: Development and design of a rescue boat prototype for SSRS
- Demonstration av en ny svensk elektrisk drivlina för sjötransporter Energimyndigheten (2020-018914)
- FoilCart: Demonstration of new foil concept for small boats.
- NG-FREEBS: Next Generation Hydrofoil System for Robust and Cost-Effective Electric Work Boats – Trafikverket (TRV 2022/108213)
- Candela's electric foiling ferry for Stockholm archipelago
- Research projects on control system development for foiling craft at Chalmers and KTH financed by Trafikverket

These projects demonstrated both the value of laboratory testing and the practical limitations of existing towing tank arrangements with regards to hydrofoil tests.

Figure 2- Model boat developed by Chalmers Master Students under supervision of RISE Maritime Centre.

The standard towing-tank configuration is primarily designed for resistance and propulsion testing of conventional hull models. Using this test rig for hydrofoils proved challenging. In previous campaigns, foil testing required extensive improvisation of mounting arrangements and measurement configurations (Figure 3). These adaptations increased test effort and cost and, in some cases, compromised measurement quality due to alignment uncertainty, and instrumentation constraints.

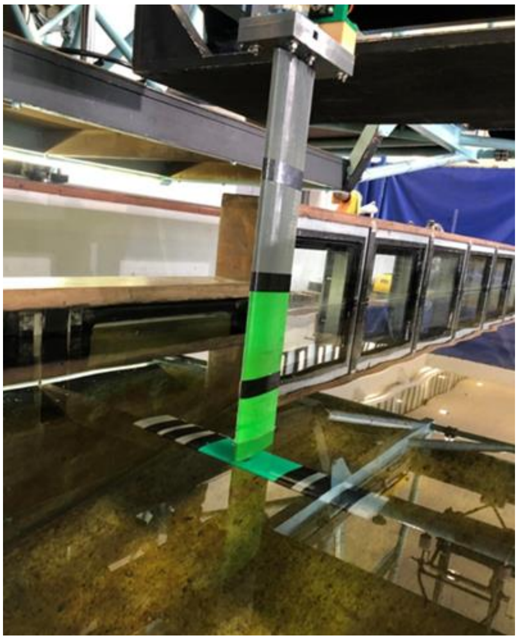

Figure 3 - Foil measurement in Towing tank [3]& [4].

Another fundamental challenge is the scaling of hydrofoil performance. Conventional model testing procedures for displacement vessels emphasize Froude similarity based on the hull length (LPP). However, hydrofoil lift and drag depend strongly on viscous and boundary-layer phenomena, making the Reynolds number critical, particularly for near surface operation, transitional flow effects, and drag components sensitive to surface roughness.

For hydrofoils operating near the free surface, the problem is inherently complex:

- Free surface interaction is governed largely by submergence Froude similarity.
- Lift and viscous drag are strongly Reynolds number dependent.

Towing tanks operate at limited maximum carriage speeds compared with the full-scale operating speeds of many foiling crafts, which complicates achieving Reynolds similarity at model scale. One practical strategy is to decouple the scaling of hull and foil systems recognizing that foiling craft operate in at least two regimes (planing and foiling) and to design experimental campaigns that explicitly address the requirements of Froude and Reynolds similarity of the foil independent of the hull. Opposite to conventional ITTC-style practice, we prioritize Reynolds scaling for foil loads and then correct for free surface effects using Froude number scaling considerations. For this method to work, we need to have dedicated test rig and accurate measurement arrangements.

Reliable hydrofoil experiments must address the difficulty of measuring forces and moments under dynamic conditions representative of real operation. Key sources of uncertainty include:

- Real-time control and measurement of foil depth (submergence), especially in waves.
- Accurate determination of foil's angle of attack.
- Capturing unsteady loads and moments arising from wave encounters.

These challenges are central for developing testing procedures that can support the next generations of active-controlled foiling craft.

To address the limitations identified in prior test campaigns, this project designed, manufactured, and used a dedicated hydrofoil testing rig for the RISE/SSPA towing tank. The rig was developed to enable measurement of all relevant force and moment components under controlled operating conditions, while supporting improved repeatability in foil positioning and attitude.

A comprehensive experimental campaign was then completed in the towing tank using the new setup. The tests focused on demonstrating the capability of the rig and establishing a practical methodology for hydrofoil performance, including:

- operation at different **foiling heights (submergence conditions)**,
- comparison using **two different foil sizes**, and
- Variable force measurement of hydrofoil in both **head waves** and **following waves**.
- Measuring the wave elevation in two locations using sonars.

The tests were conducted to evaluate the performance and suitability of the testing platform as a foundation for future systematic towing-tank investigations of hydrofoils and foiling craft components.

1.3 Power Requirement in Foiling Vessels

Foiling vessels operating at higher speeds generate only a fraction of the wave system produced by displacement vessels of similar tonnage. In addition, their wetted surface area is significantly smaller than that of displacement or planing hulls. Together, these factors result in a substantial reduction in hydrodynamic drag for foiling vessels. Figure 4 put the power reduction for light vessels in cruising speed of 40kn close to 80%. (see www.flying-fish.tech/hydrofoils)

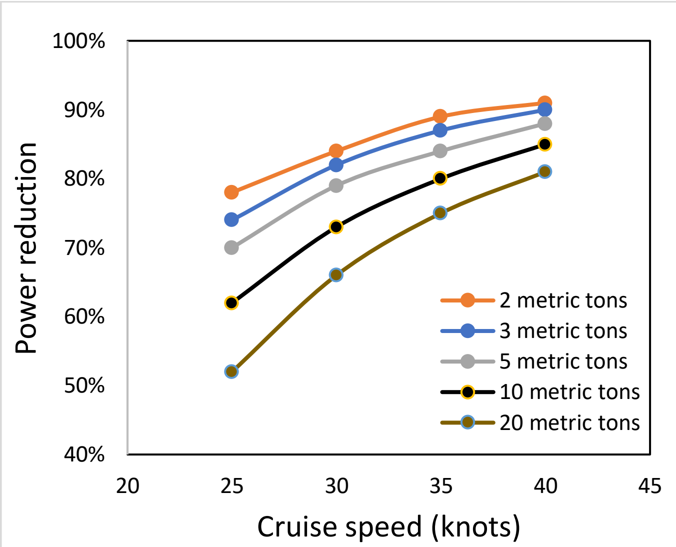

Figure 4 - Typical power reduction comparison between planing and foiling boat (flying-fish.tech/hydrofoils)

To initiate the propulsion unit selection process, the vessel's speed-resistance and speed-loading characteristics must first be evaluated. This is inherently an iterative process, as both the choice of propulsion system and the hydrofoil configuration have a significant influence on the overall vessel resistance. Figure 5 illustrates a representative resistance–speed relationship for a typical foiling vessel [5].

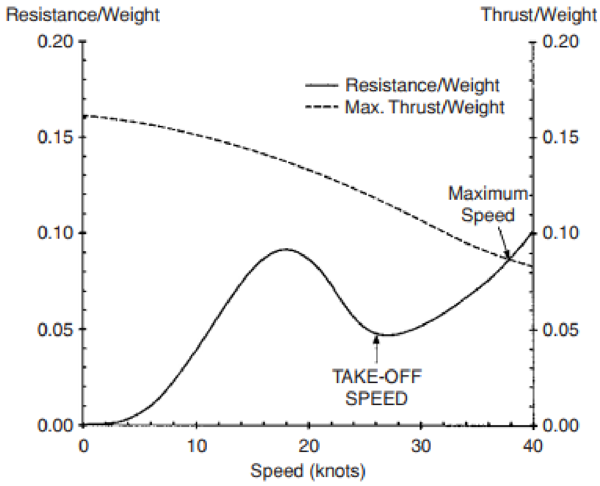

Figure 5- Example of resistance and thrust versus speed [5].

1.4 Theory of the Hydrofoiling Vessel

A vessel moving through water experiences resistance from the displaced fluid in the form of hydrodynamic pressure forces and frictional resistance. When the motion occurs at the interface between air and water, additional pressure disturbances are generated at the free surface as gravitational waves that interact with the vessel. If the vessel speed exceeds the propagation speed of these surface waves, hydrodynamic forces tend to lift the vessel further into the phase with lower resistance, namely air.

For high-speed vessels, this regime corresponds to the planing mode, in which the hull is partially lifted out of the water by pressure forces acting on the bottom of the hull. Planing hulls are designed to operate efficiently at higher speeds by reducing wetted surface area and adjusting trim. In this case, lift is generated primarily by dynamic pressure on the hull bottom, while the upper surfaces are exposed to lower air pressure.

Foiling vessels also reduce resistance by generating lift and pushing the hull out of the water. The fundamental distinction between planing and foiling vessels lies in the source of this lift. In foiling craft, lift is primarily generated by dedicated lifting appendages, the hydrofoils, which support the vessel during the foiling phase of operation, thereby minimizing hull-water interaction and associated resistance.

The weight of the vessel is balanced by the steady lift force from the horizontal hydrofoil system in the foilborne condition (see Faltinsen [5]):

$$M.g = \frac{\pi}{2}\,\rho\,A\,C_L U^2$$

where M is the mass of the vessel, A is the plan area of the hydrofoil, C_L is the coefficient of the lift and U is the vessel speed.

Another difference between a displacement vessel and a foiling vessel lies in the choice of characteristic dimensionless parameters that describe the governing flow regime. For conventional displacement vessels, the Froude number, defined using the vessel length scale, is used to characterize the vessel speed relative to the propagation of free surface waves. In contrast, if the struts connecting the hydrofoils to the hull are neglected, a foil borne vessel effectively operates in two distinct fluid regions, with most free surface disturbances generated by the submerged hydrofoil rather than the hull. Consequently, the submergence-based Froude number, defined using the foil depth below the free surface as the characteristic length scale, becomes the more relevant parameter for describing the hydrodynamics of foiling vessels:

$$Submergence\ Froude\ number: \qquad Fn_h = \frac{U}{\sqrt{gh}}$$

where *h* is the submergence of the hydrofoil. The wave resistance of the foiling vessel is characterized by its submergence Froude number.

In deep water, submergence ratio, together with the Reynolds number define the lift coefficient of the hydrofoil:

$$Submergence\ ratio: \qquad \frac{C}{h}$$

$$Reynolds\ number: \qquad Re = \frac{C.U}{\nu}$$

where *C* is the maximum chord length of the main foil.

1.5 Free Surface Effects on a Foil

As a hydrofoil operates closer to the free surface, its lift progressively decreases. At shallower submergence, the interaction with the free surface intensifies, leading to increased wave generation and a corresponding rise in total foil drag. Velinga [1] characterizes this effect through a "submergence factor," defined in terms of the foil chord length CCC and the foil submergence depth *h*, given as follows:

$$Submergence\ Factor: \qquad F_s = 1 - 0.222\left(\frac{1.5\ C - h}{C}\right)^2 \qquad ; for\ \frac{h}{C} < 1.5$$

$$F_s = 1 \qquad ; for\ \frac{h}{C} \geq 1$$

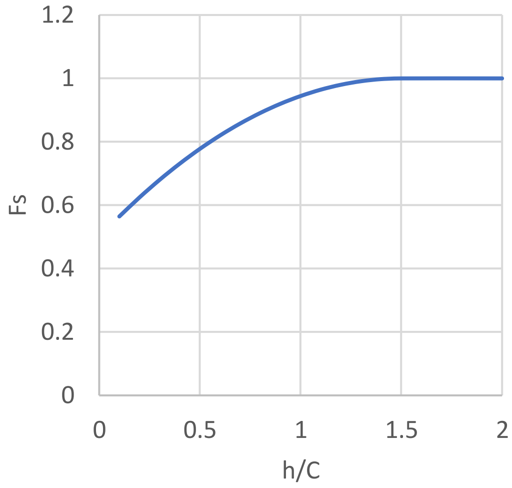

Figure 6-Submergence Factor Fs

And the lift force can be calculated as:

$$Lift = \frac{\pi}{2}\,\rho\,A\,C_L U^2\,F_s$$

The surface effect can contribute to pitch stability, and a control system should be used to compensate for the effect. In most foil designs, operating deeper than one chord length (Submergence ratio > 1) is favorable. Foiling close to the surface also increases the risk of ventilation, which has a negative effect on the foil.

In some hydrofoil designs, the Submergence Factor (F_s) can be used as a passive height stability controller, as increase in speed results in higher lift, which results in that hydrofoil approaches the free-surface and loses its lift.

Faltisen [5] in his work presents how the proximity of free surface modifies the hydrodynamic performance of a submerged hydrofoil. Unlike a foil operating in an unbounded fluid, a hydrofoil beneath a free surface experiences changes in lift, additional wave making drag, and a complex dependence on the submergence Froude number. Understanding these effects is essential for hydrofoil vessel design, where foils typically operate at submergences on the order of one to a few chord lengths and at speeds corresponding to Froude numbers well above unity.

As foil geometry is not intrinsically tied to its operating depth, two independent length scales are introduced for hydrofoil analysis. The first is the chord length, C, which governs the geometric scaling of the foil and is used to form the Reynolds number and the nondimensional lift and drag coefficients. The second is the submergence depth, h, defined as the characteristic vertical distance between the foil and the free surface. Because hydrofoil motion in proximity to the free surface can generate gravity waves and associated wave-making effects, a submergence Froude number is also defined to quantify the effect the free surface interaction.

The submergence Froude number Fn_h governs the character of free surface interaction. Linear wave theory gives the wavelength of foil generated waves as $\lambda = 2\pi U^2/g$, and the induced flow beneath the free surface decreases for the operating depth on the order of λ. Consequently, wave generation becomes significant when

$$Fn_h > \frac{1}{\sqrt{2\pi}} \approx 0.4$$

Below this threshold, free surface effects are negligible. Above it, wave generation substantially alters the lift, with strong variations persisting up to approximately $Fn_h \approx 10/\sqrt{h/c}$ or $U/\sqrt{g/c} \approx 10$. When $Fn_h > 10/\sqrt{h/c}$, the lift coefficient C_L is nearly independent of Fn_h. Beyond this value the gravitational restoring force becomes negligible on the time scale of the flow.

Figure 7 shows an example of lift coefficient variation (C_L of a hydrofoil operating in different submergence to chord length ratio h/C, compared to the foil operating in finitely deep water).

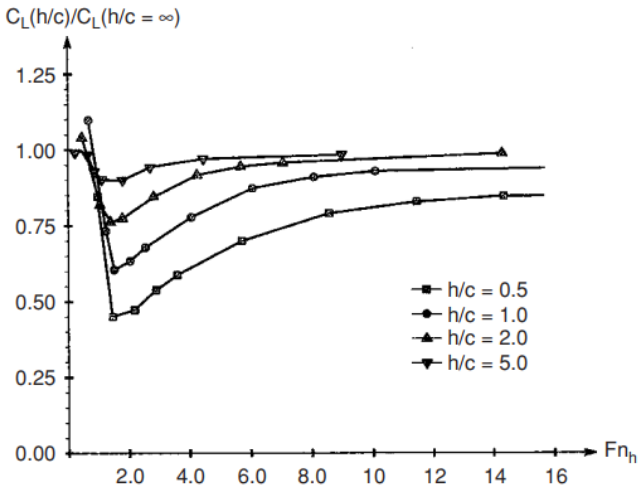

Figure 7 - The Lift Coefficient variation of a 2D hydrofoil due to proximity to the free surface. [5]

When the Froude number is very small, the condition could be described as a lifting wing close to the ground (ground effect wing) and the lift coefficient slightly increases with decreasing depth. A foil operating sufficiently close to the free surface generates steady downstream waves and therefore experiences a wave resistance. Using potential flow formulation, the wave resistance due to lift effects on a 2D foil is expressed as

$$\frac{C_{DW\Gamma}}{C_L^2} = \frac{0.5}{Fn_h^2}\left(\frac{c}{h}\right) \exp\left(-\frac{2}{Fn_h^2}\right)$$

This ratio peaks at $Fn_h = \sqrt{2}$, with maximum value $0.25\ e^{-1}\ c/h = 0.092\ c/$

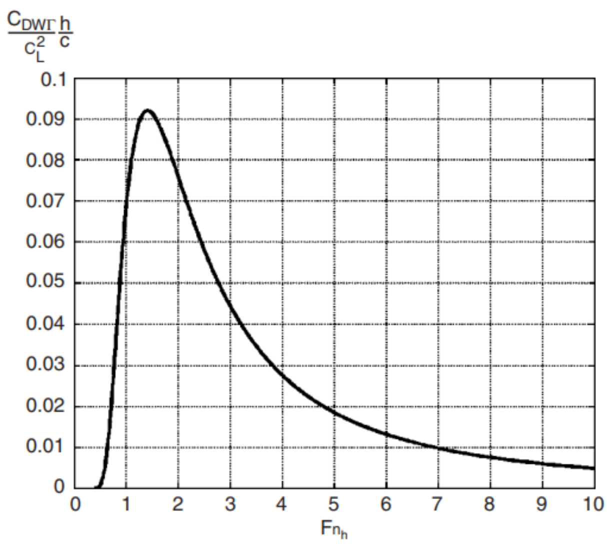

Figure 8 - Wave resistance of a 2D foil operating near free surface [5].

In all these formulas we assumed a 2D foil and neglected the wing-tip effect and spanwise load variation of a real 3D hydrofoil. The strut-foil interaction, strut-free surface interaction and strut ventilation are the effects which are not considered in an idealistic 2D foil.

1.6 Foil Loding and Power Calculation

To start the selection process for the propulsion unit, we must look at the speed-loading of the foil system. The main foil of the vessel produces the necessary lift based on the speed of the vessel and the angle of attack. Also to avoid cavitation, the main foil operates in a limited region of the lift-speed curve. Using this information, we can define boundaries for the vessel speed and the steady foil loading that the vessel must operate within. We then add sea margin to account for unsteady wave effects. Figure 9Figure 9 presents the graph for two different NACA 16 series hydrofoils (see Faltinsen [5]).

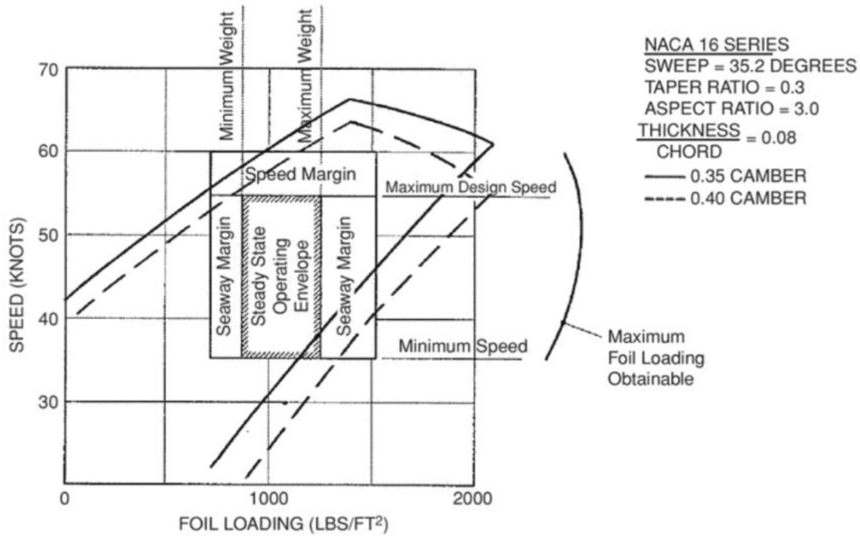

Figure 9- Foil loading-speed envelope for two different foil sizes of NACA16 series.

A key design consideration is ensuring that the propulsion system provides sufficient power and efficiency to enable the vessel to transition from planing to foiling. As speed increases in the planing regime, the hull trim angle typically increases, which in turn raises the angle of attack of the main foil. While this effect can facilitate earlier take-off, it may also increase induced drag on the main foil, potentially preventing the vessel from reaching the required foiling speed. This interaction should therefore be accounted for when estimating the required propulsion power.

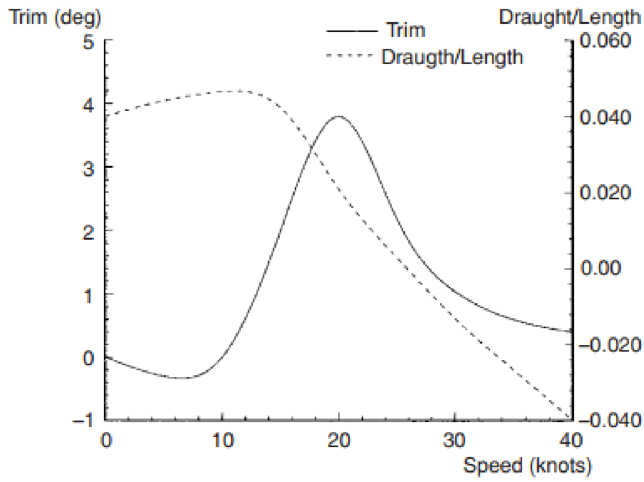

Figure 10 – Typical example of draught and trim angle variation during take-off sequence [5].

1.7 Foil Configuration and Design Parameters

The parameters for designing a foiling vessel include the vessel displacement, the maximum foil-borne operating speed, and the take-off speed. The intended operational profile further influences the selection of foil size and geometry. For an individual foil system, in addition to the basic geometric shape of the foil, the following parameters are considered central to the design process:

- Angle of attack of the incident flow
- Flap angle
- Camber
- Thickness to chord ratio
- Aspect Ratio of the foil
- Submergence ratio
- Submergence Froude number
- Foil cavitation number
- Foil Reynolds number

There are two principal categories of hydrofoil vessels: fully submerged foil systems and surface-piercing foil systems. The stability of a hydrofoiling vessel is strongly influenced by its weight distribution and the arrangement of the lifting foils. The vessel's weight may be primarily supported by either a forward or an aft foil, commonly referred to as the **main foil**, while the secondary foil—often called the **elevator**—is used to control trim and longitudinal balance. An alternative configuration is the tandem foil arrangement, in which the vessel's weight is distributed between both the forward and aft foils to achieve overall stability and control. (see Figure 11)

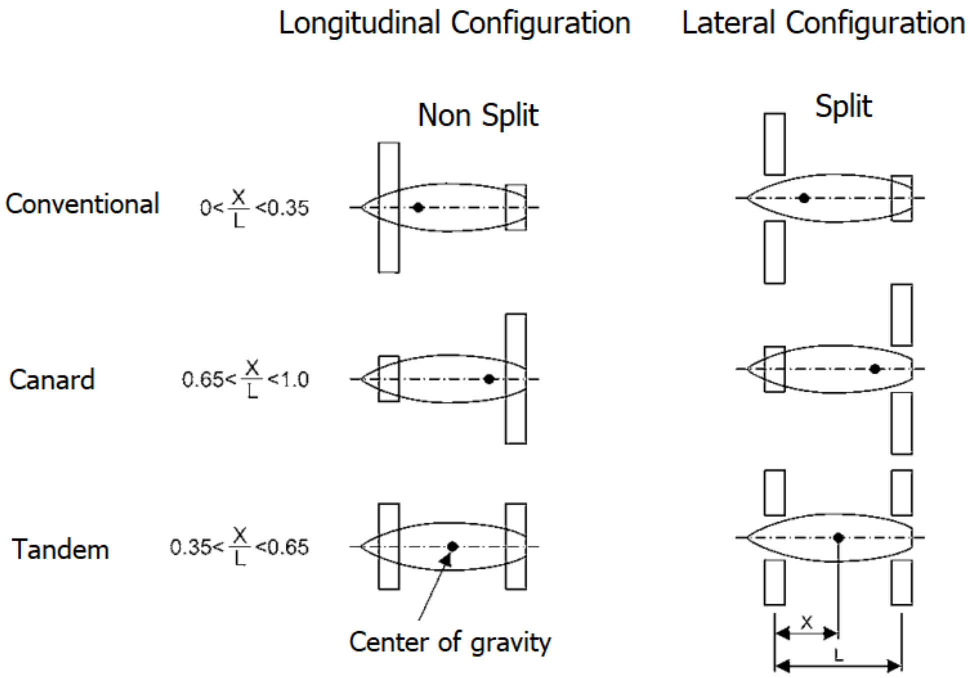

Figure 11 - Hydrofoil configuration [5].

2 Design and Integration of Test Rig

RISE/SSPA towing tank is equipped with a carriage with a platform for mounting different measurement equipment. Figure 12 shows the structure of the platform on the carriage.

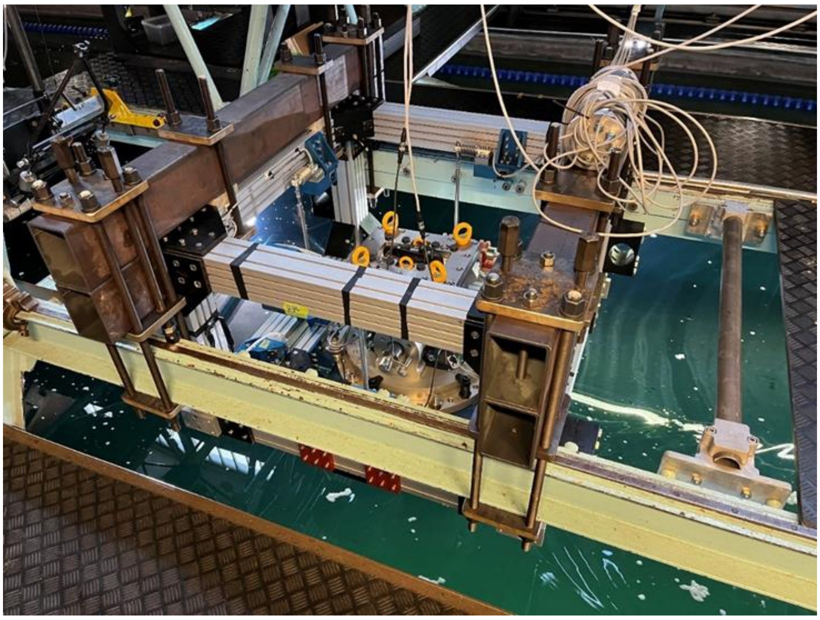

Figure 12 - Towing tank carriage rails available for the testing rig.

The measurement rig consists of two parts. An outer frame provides the primary rigid structure and incorporates fixtures for connection to the towing carriage platform. Within this frame, an inner platform is suspended by four rods, each connected to force and moment measurement gauges. The inner platform has a light blue color in Figure 13 inside the outer frame.

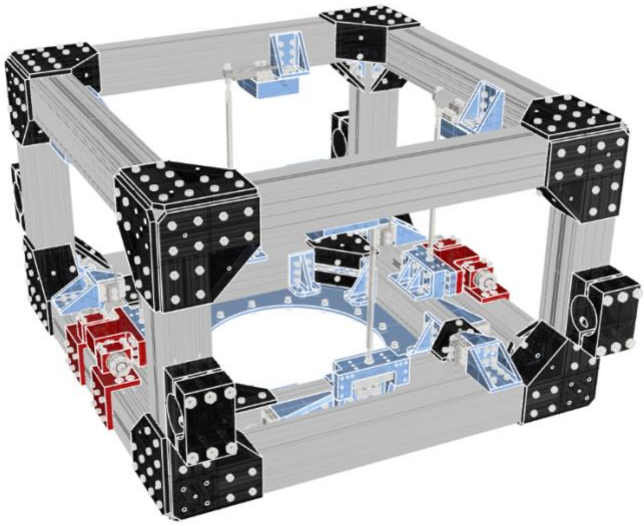

Figure 13 - Outer frame with suspended cage for the force and moment cells gauges.

To attach the hydrofoil to the measurement rig, a configurable mounting assembly was developed, providing two rotational degrees of freedom (Figure 14). The foil strut is clamped within a sliding carriage, and interchangeable sleeves integrated into the mounting block accommodate different strut cross-sections and sizes.

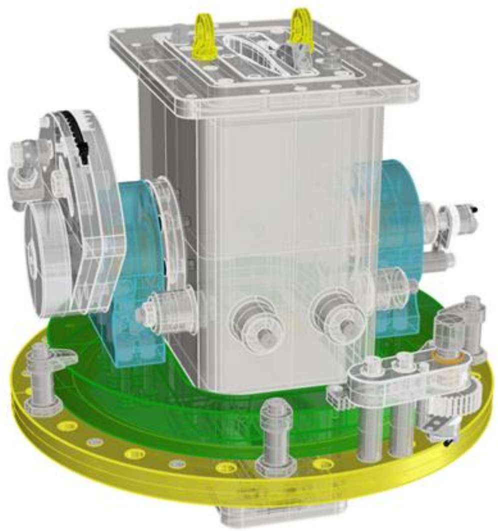

Figure 14 - Foil mounting section with 3 degrees of freedom adjustment (pitch, height and yaw).

Two different types of hydrofoils were installed inside the mounting section as shown in Figure 15.

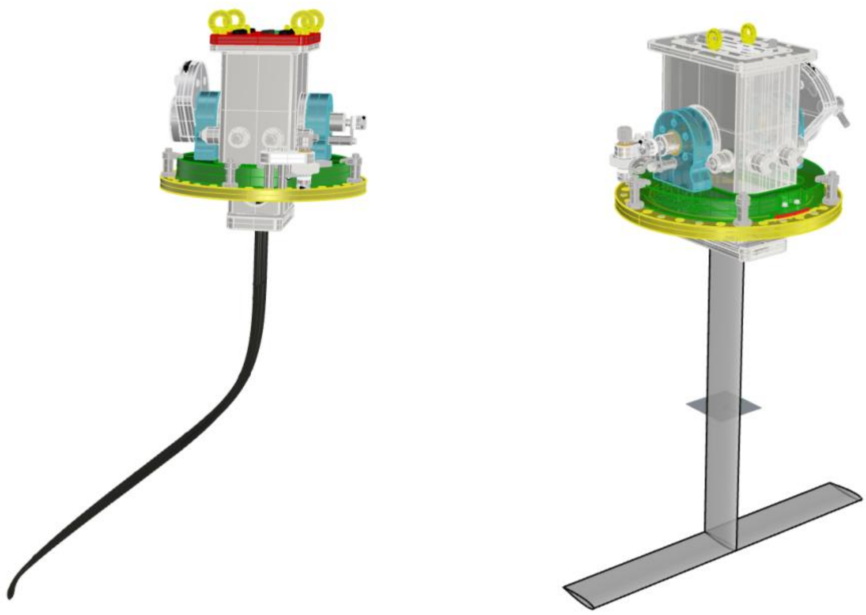

Figure 15 - Nacra 17 and T-foil installed in mounting section

The complete setup of the measurement rig is presented in the Figure 16 with a generic T-foil.

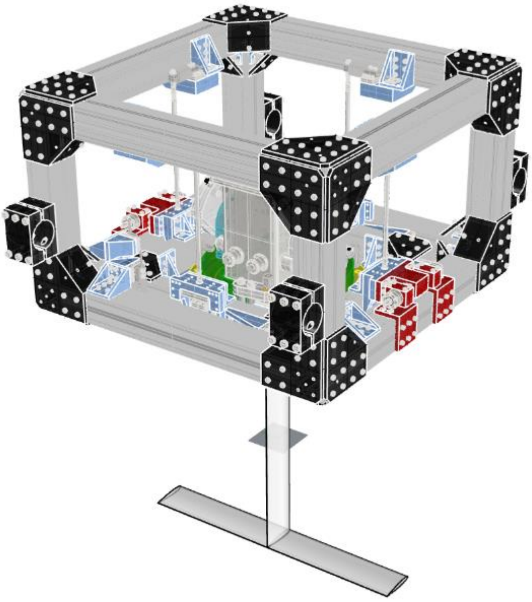

Figure 16 - Schematic of the test rig and a foil installed.

We performed a series of tests in towing tank using the designed rig. Figure 17 is a snapshot of the test rig and the foil during the test.

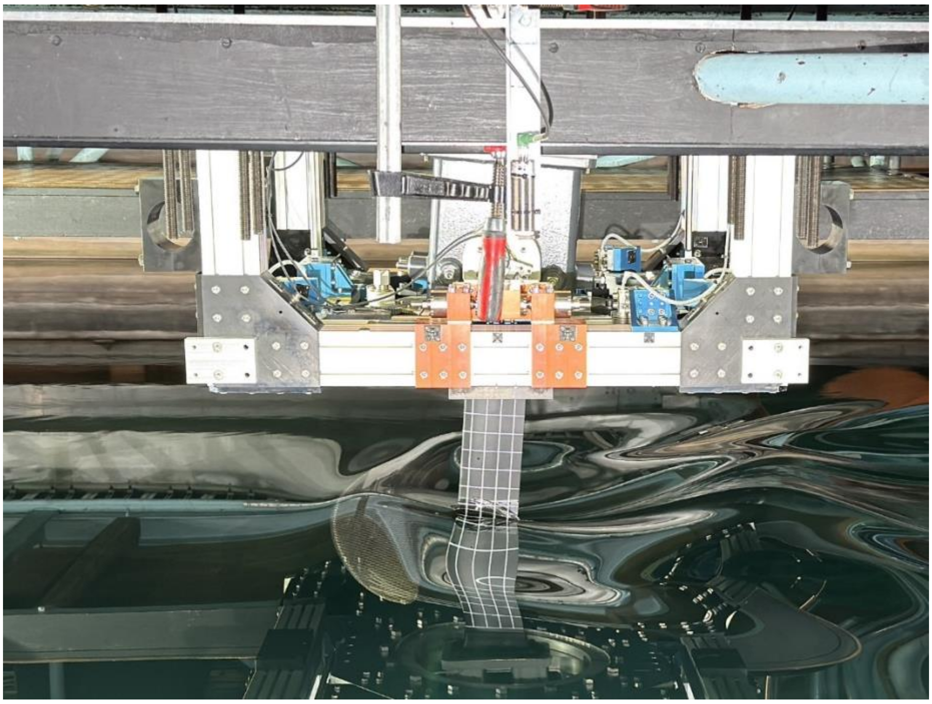

Figure 17- Test rig and hydrofoil installed under the carriage.

3 Tested Hydrofoil Specifications

To evaluate the testing rig's performance and measurement capability, a test campaign was carried out with two commercially available hydrofoils. During the search for a manufacturable hydrofoil suitable for systematic scaling, we identified a range of commercially available foils originally developed for foiling boards. In particular, the Gong Galaxy wings are offered in multiple sizes. A key advantage of this product line is that the foils share a common geometry, and the different sizes represent geometrically scaled variants of the same baseline design, which makes them well suited for comparative testing across different scales.

Small Foil - gong-galaxy, Wing Curve H v2		
Chord Length	118	mm
Wingspan	770	mm
Wingspan^2/surface area ratio	8.4	
Thickness	15	mm
Volume	0.57	lit
Projected area	702	cm^2

Large Foil - gong-galaxy, Wing Curve H v2, 3XL		
Chord Length	191	mm
Wingspan	1250	mm
Wingspan^2/surface area ratio	8.4	
Thickness	24	mm
Volume	2.43	lit
Projected area	1850	cm^2

Wing geometries are the scaled with the scale factor of 1:1.618 with the exception of mounting section at the center of wing. Both wings were fabricated from carbon fiber laminations (Figure 18) and have a common mounting interface to an aluminum strut. As a result, foils can be exchanged quickly between runs, minimizing downtime and eliminating the need for repeated adjustments.

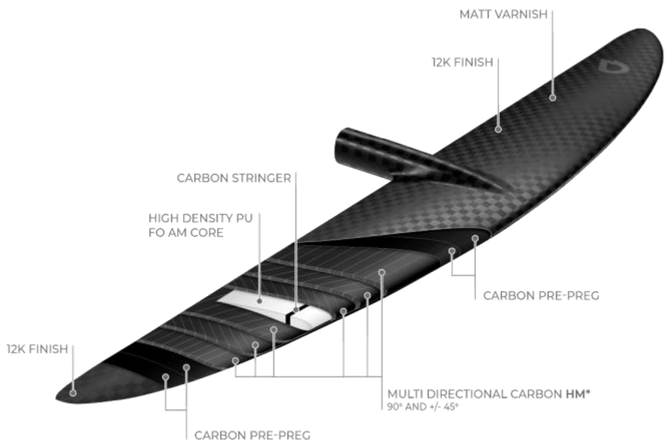

Figure 18- Gong Galaxy wing foil, manufactured with layers of carbon fibre.

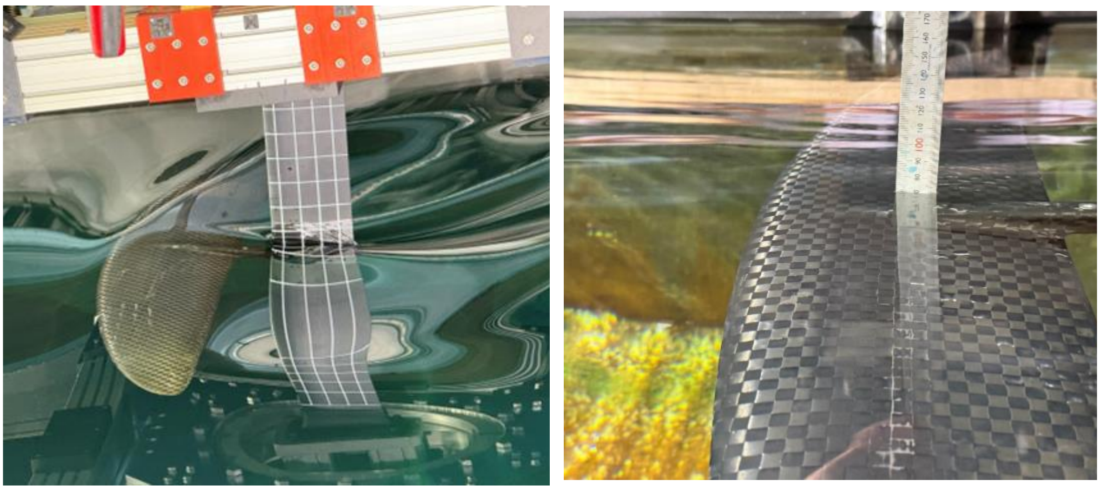

Figure 19 - Foil and strut connection.

The placement of connecting joint to the strut was behind the foil as shown in Figure 19. To set a non-zero angle of attack, the strut was rotated within the mounting block. Because the strut axis was located aft of the wing's rotational centre, pitching the foil to the target angle of attack also altered its submergence depth. Consequently, the foil submergence was measured after each adjustment while the system was held stationary.

To enable the use of foil geometry in CFD simulations, the wings were digitized using a 3D scanner and the corresponding CAD surfaces were reconstructed. Figure 20 shows the resulting three-dimensional CAD model of the scanned wing assembly, including the strut and fuselage. In addition, a streamlined conical fairing was manufactured and mounted at the aft end of the fuselage to reduce the overall drag of the foil system.

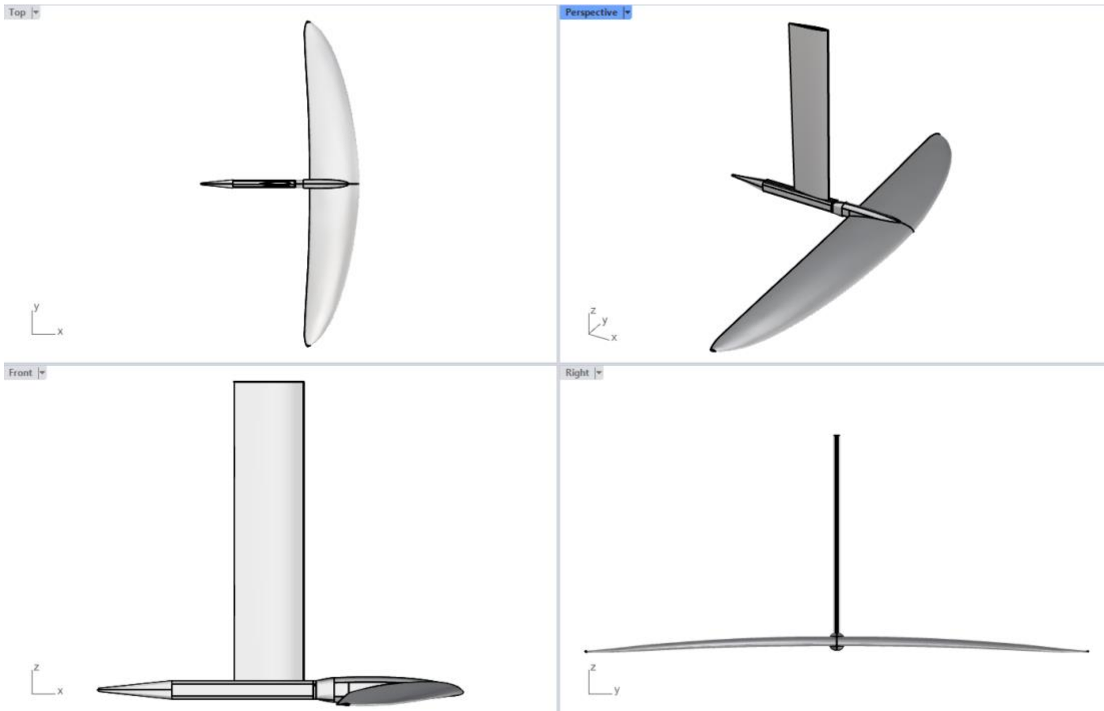

Figure 20- Reconstructed CAD model from 3D scanned wings.

The wing shows a varying chord length in spanwise direction, an angle of attack at the root, and a slight anhedral configuration.

4 Performed Tests

As a part of the project, we performed a series of different tests using the manufactured rig in RISE/SSPA towing tank.

The primary objectives of these tests were to:

- Identify and map the key factors influencing hydrofoil performance evaluation in a towing tank test.
- Determine the operational and measurement limits of the rig across representative test conditions.
- Generate baseline data for subsequent comparison with CFD predictions.

4.1 Measurement Equipment and Data Acquisition

The test rig is capable of measuring three force components (Fx, Fy, Fz) and three moment components (Mx, My, Mz). The mounting section is capable of adjusting the foil's submergence depth and changing in the pitch angle of the foil by raking the foil mast.

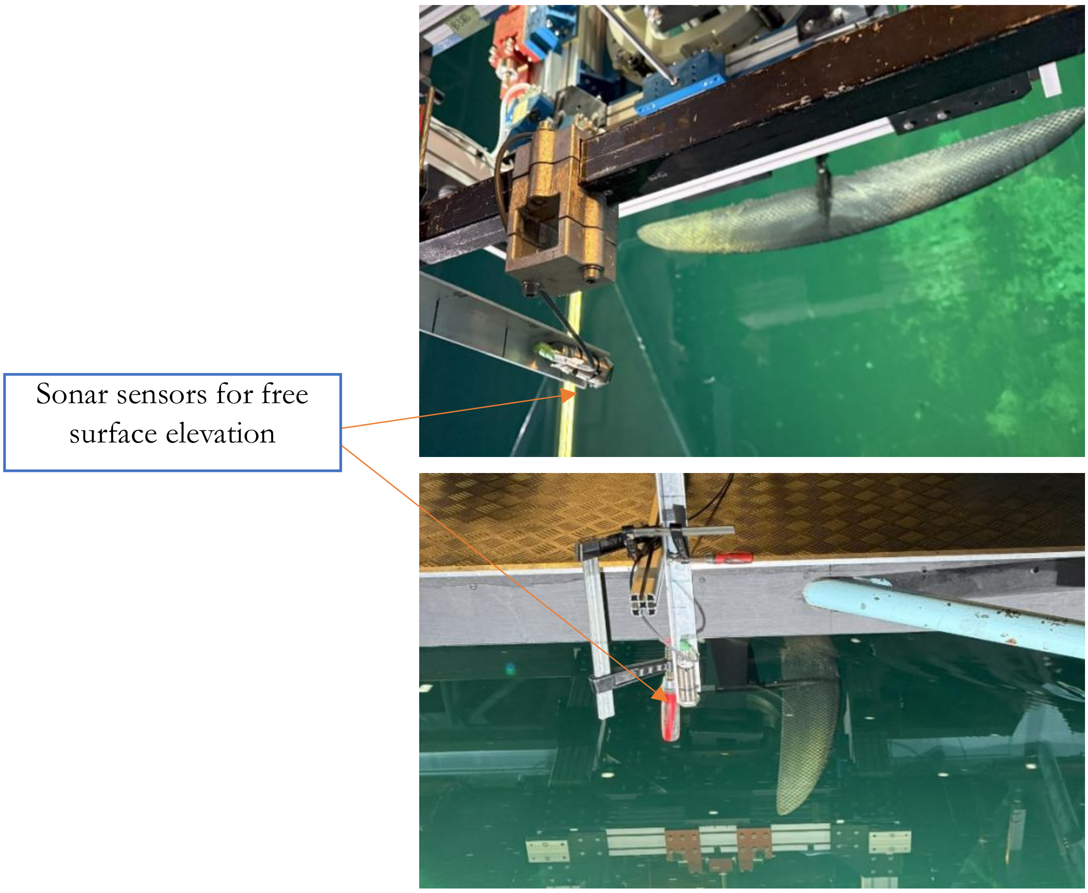

Figure 21- Position of water surface sonars, measuring the water level in front and side of the foil.

To measure the free surface elevation, two sonar sensors were installed to track the water surface position. These measurements are used to monitor the local wave height during tests conducted in waves. Figure 21 illustrates the locations of the sonar sensors relative to the mounted foil. The sensors were positioned 1000 mm upstream of the foil mast centre and 1480 mm laterally from the mast centreline for the measurements in following waves.

Regular waves were generated by the wavemaker at the end of the towing tank and propagated toward the upstream end of the basin. Accordingly, two wave-test configurations were implemented: head-wave tests, in which the foil encountered the oncoming waves, and following-wave tests, in which the foil travelled in the same direction as wave propagation. For head-wave conditions, the foil was oriented toward the incoming wave train and the carriage traversed toward the wavemaker. For following-wave conditions, the carriage run was initiated near the wavemaker end of the basin, and data acquisition started as the carriage moved toward the upstream end, i.e., in the direction of wave propagation (Figure 22).

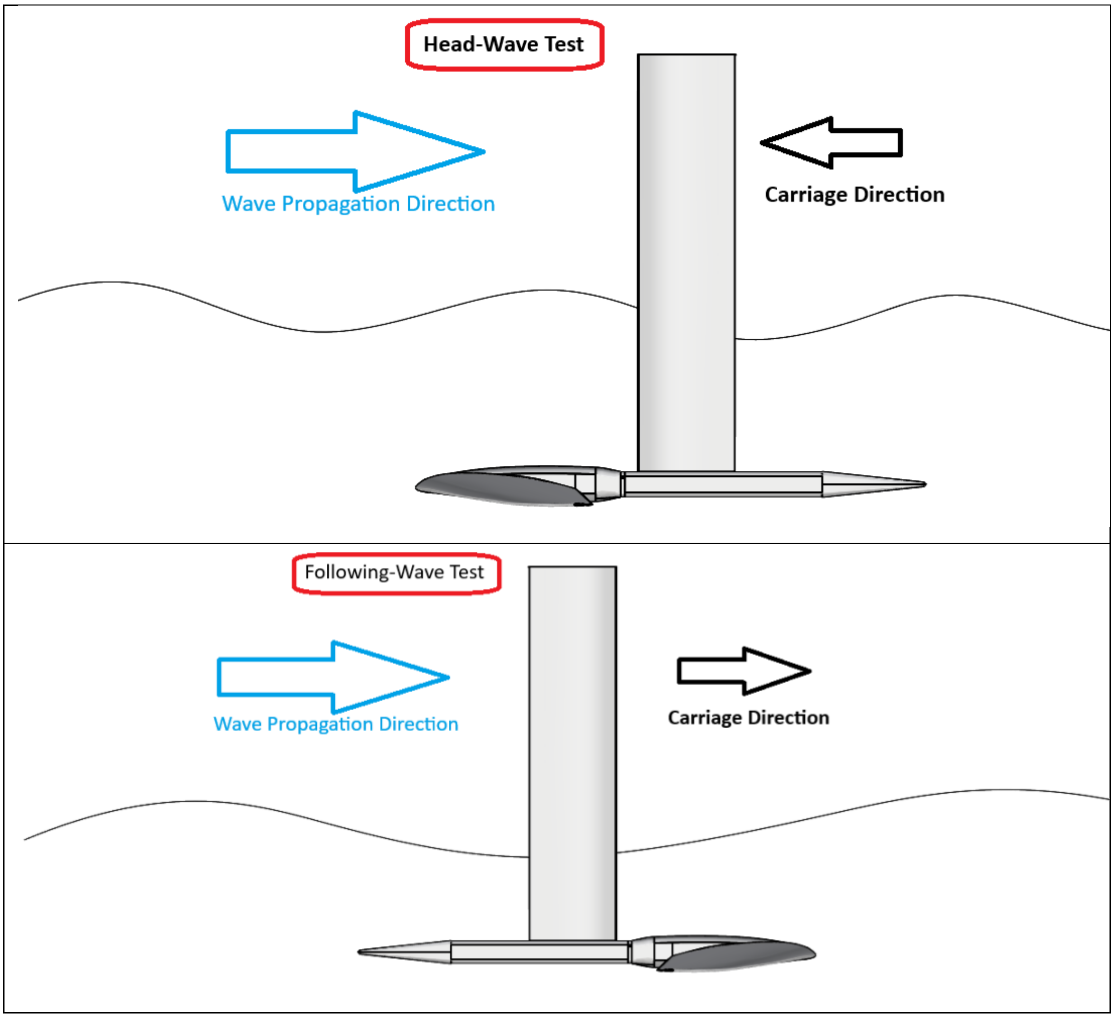

Figure 22 - The head-wave and following-wave test configuration.

In the test series involving non-zero angle of attack, the entire foil mast was pitched forward. As illustrated in Figure 23, this adjustment also altered the foil submergence. Consequently, the foil position relative to the free surface was measured and recorded for each test series.

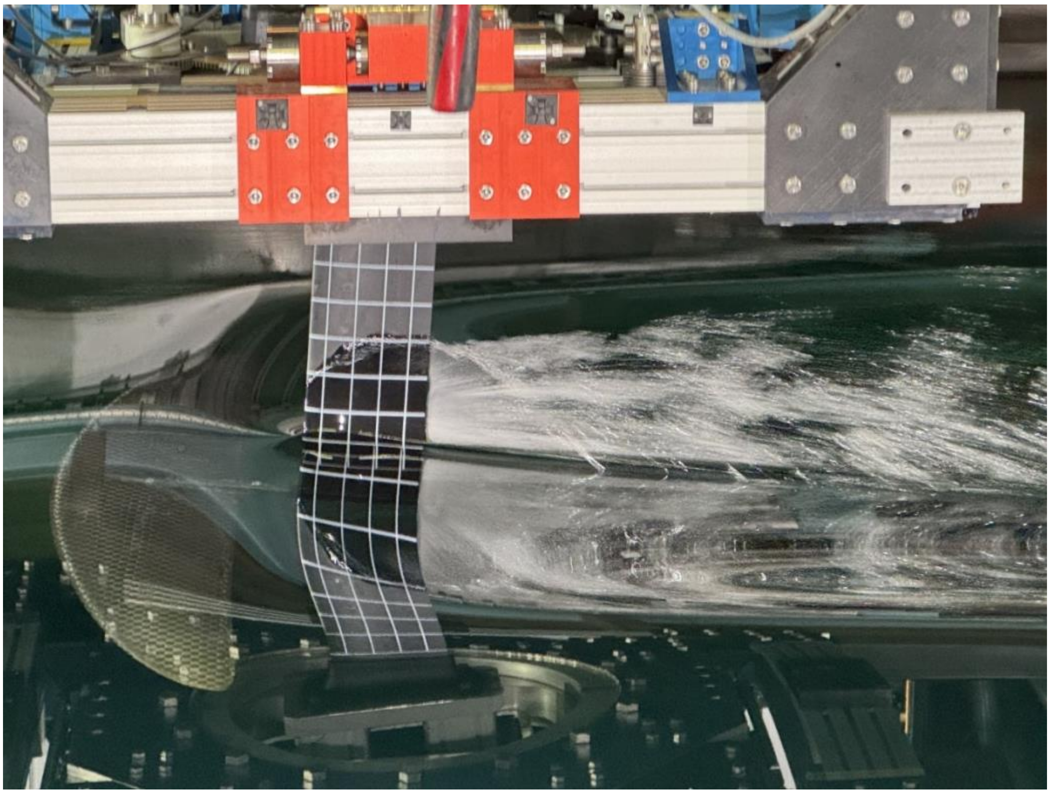

Figure 23- Tests with non-zero angle of attack.

4.2 Test Series

Following the test setup described above, a total of **eight** test series were conducted. **Six** series were performed under **calm water** conditions, while **two** series were conducted in waves: one in **head seas** and one in **following seas**. Two of the calm water series used the **small hydrofoil**; all remaining series, including both wave campaigns, were carried out with the **large hydrofoil**.

For the **small foil** measurements, the submergence was kept constant at $H/C = 1.7$. Two angles of attack were tested: $\alpha = 0°$ for one series and $\alpha = 4°$ for the other.

A dedicated **submergence variation** series was performed using the **large hydrofoil** at $\alpha = 4°$. The **wave condition** measurements were also conducted with the large foil and were executed at a constant submergence of $H/C = 2$ and $\alpha = 4°$.

The experimental setup and the resulting force measurements are described in the following sections.

4.3 Series 1 – Calm Water – Small Foil – Angle of Attack 4 deg

This calm water test series used the **small hydrofoil**. The **lift and drag forces** acting on the complete foil system, comprising the **wing (foil), fuselage, and mast,** were measured. The corresponding **test conditions** and **foil specifications** are summarized in Figure 24.

Test condition		
Depth	200	mm
H/C	1.7	
AoA	4	deg
Wave condition	calm	
Wavelength	0	m
Wave height	0	mm

Small Foil - gong-galaxy, Wing Curve H v2		
Chord Length	118	mm
Wingspan	770	mm
Wingspan²/surface area ratio	8.4	
Thickness	15	mm
Volume	0.57	lit
Projected area	702	cm²
Extrados area	727	cm²
Felt area	700	cm²

Figure 24 - Test Series 1 tables of specifications.

Tests were conducted at a constant submergence depth of 200 mm, while the towing speed was varied up to 10 m/s. Lift and drag forces were recorded across the tested speed range. The measured lift increased with speed and reached approximately 2 kN at 10 m/s (Figure 25).

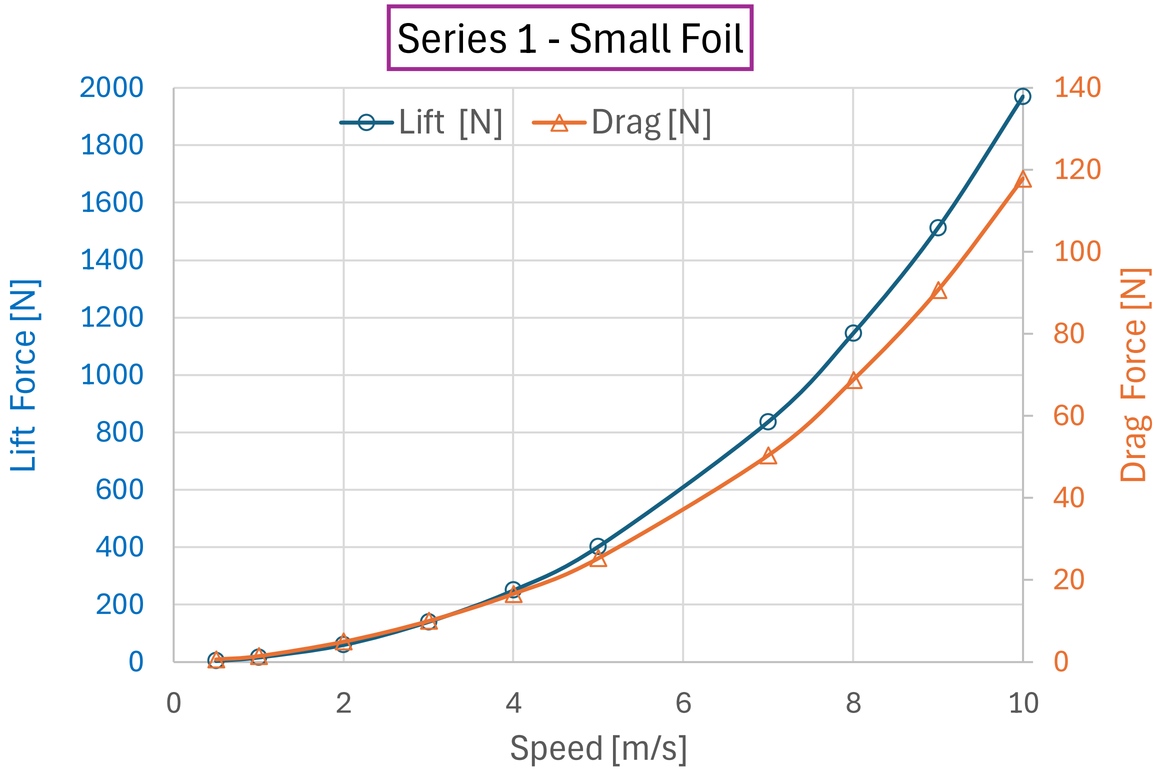

Figure 25- Series 1- Lift and Drag forces measured in calm condition.

4.4 Series 2 – Calm Water – Small Foil – Angle of Attack 0 deg

This calm water test series used the **small hydrofoil**. The **lift and drag forces** acting on the complete foil system, comprising the **wing (foil), fuselage, and mast,** were measured. The corresponding **test conditions** and **foil specifications** are summarized in Figure 26.

Test condition		
Depth	200	mm
H/C	1.7	
AoA	0	deg
Wave condition	calm	
Wavelength	0	m
Wave height	0	mm

Small Foil - gong-galaxy, Wing Curve H v2		
Chord Length	118	mm
Wingspan	770	mm
Wingspan²/surface area ratio	8.4	
Thickness	15	mm
Volume	0.57	lit
Projected area	702	cm²
Extrados area	727	cm²
Felt area	700	cm²

Figure 26- Test Series 2 tables of specifications.

Tests were conducted at a constant submergence depth of 200 mm, while the towing speed was varied up to 10 m/s. Lift and drag forces were recorded across the tested speed range. The measured lift increased with speed and reach approximately 836N at 10 m/s (Figure 27).

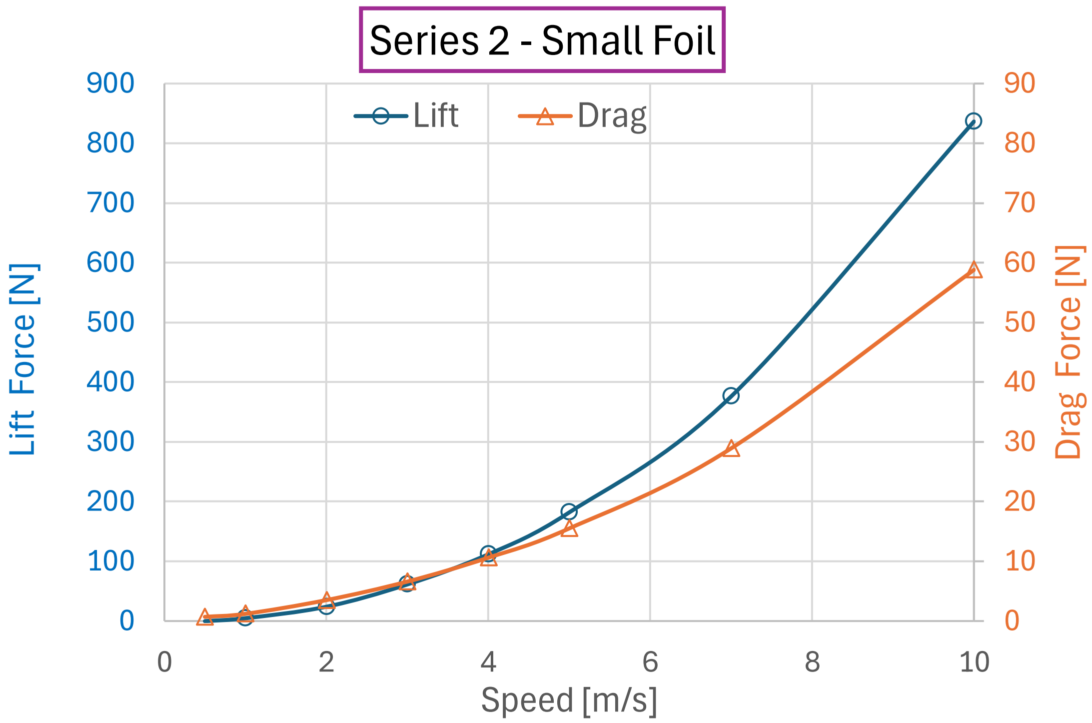

Figure 27- Series 2- Lift and Drag forces measured in calm condition.

4.5 Series 3 – Calm Water – Large Foil – Submergence 200mm – AoA 4°

This calm water test series used the **large hydrofoil**. The **lift and drag forces** acting on the complete foil system, comprising the **wing (foil), fuselage, and mast,** were measured. The corresponding **test conditions** and **foil specifications** are summarized in Figure 28.

Test condition		
Depth	200	mm
H/C	1.04	
AoA	4	deg
Wave condition	calm	
Wavelength	0	m
Wave height	0	mm

Large Foil - gong-galaxy, Wing Curve H v2, 3XL		
Chord Length	191	mm
Wingspan	1250	mm
Wingspan²/surface area ratio	8.4	
Thickness	24	mm
Volume	2.43	lit
Projected area	1850	cm²
Extrados area	1918	cm²
Felt area	1850	cm²

Figure 28- Test Series 3 tables of specifications.

Tests were conducted at a constant submergence depth of 200 mm, while the towing speed was varied up to 6 m/s. The measured lift increased with speed and reached approximately 2.2kN at 6 m/s (Figure 29). Due to the excessively high lift loads and their impact on measurement reliability, 6 m/s was selected as the maximum test speed for the large foil.

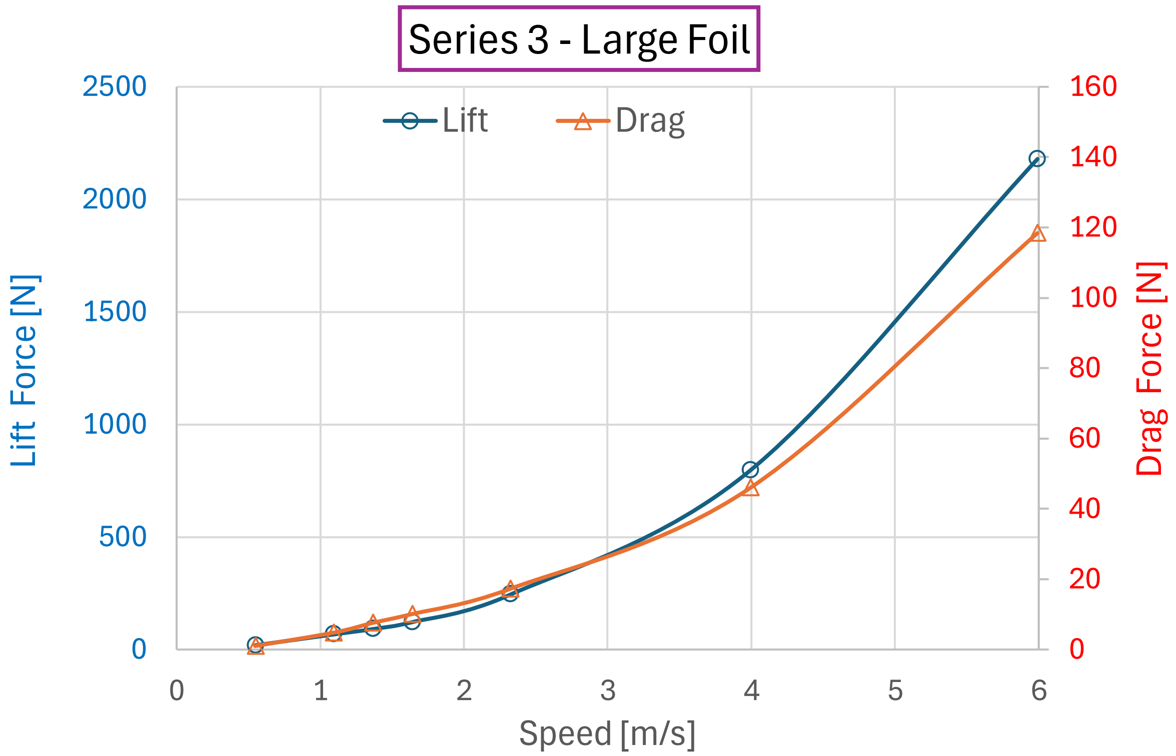

Figure 29- Series 3- Lift and Drag forces measured in calm condition.

4.6 Series 4 – Calm Water – Large Foil – Submergence 400mm – AoA 4°

This calm water test series used the **large hydrofoil**. The **lift and drag forces** acting on the complete foil system, comprising the **wing (foil), fuselage, and mast,** were measured. The corresponding **test conditions** and **foil specifications** are summarized in Figure 30.

Test condition		
Depth	400	mm
H/C	2	
AoA	4	deg
Wave condition	Calm	
Wavelength	0	m
Wave height	0	mm

Large Foil - gong-galaxy, Wing Curve H v2, 3XL		
Chord Length	191	mm
Wingspan	1250	mm
Wingspan²/surface area ratio	8.4	
Thickness	24	mm
Volume	2.43	lit
Projected area	1850	cm²
Extrados area	1918	cm²
Felt area	1850	cm²

Figure 30- Test Series 4 tables of specifications.

Tests were conducted at a deeper submergence depth of 400 mm, while the towing speed was varied up to 6 m/s. The measured lift increased with speed and reached approximately 3kN at 6 m/s (Figure 31). Due to the excessively high lift loads and their impact on measurement reliability, 6 m/s was selected as the maximum test speed for the large foil.

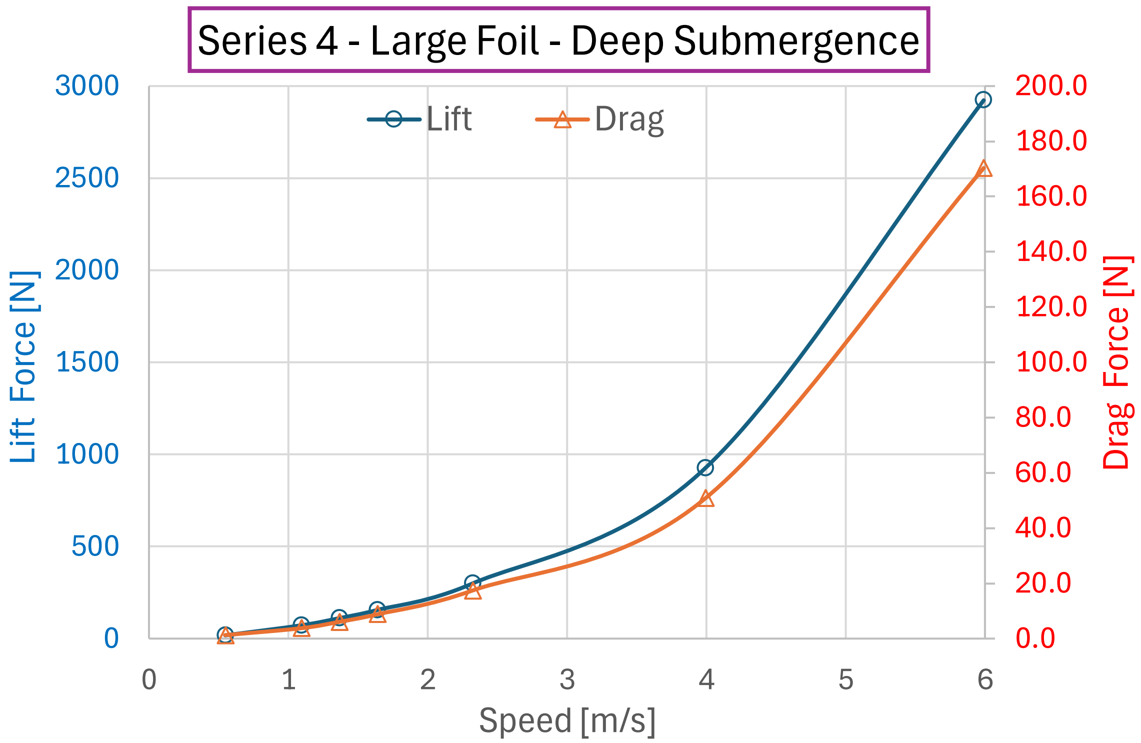

Figure 31- Series 4- Lift and Drag forces measured in calm condition.

4.7 Series 6 – Calm Water – Large Foil - Submergence 60 mm – AoA 4°

This calm water test series used the **large hydrofoil.** The **lift and drag forces** acting on the complete foil system, comprising the **wing (foil), fuselage, and mast,** were measured. The corresponding **test conditions** and **foil specifications** are summarized in Figure 32.

Test condition		
Depth	60	mm
H/C	0.31	
AoA	4	deg
Wave condition	calm	
Wavelength	0	m
Wave height	0	mm

Large Foil - gong-galaxy, Wing Curve H v2, 3XL		
Chord Length	191	mm
Wingspan	1250	mm
Wingspan²/surface area ratio	8.4	
Thickness	24	mm
Volume	2.43	lit
Projected area	1850	cm²
Extrados area	1918	cm²
Felt area	1850	cm²

Figure 32 - Test Series 6 – tables of specifications.

Tests were conducted at an extreme shallow submergence 60 mm, while the towing speed was varied up to 2.3 m/s. The measured lift and drag forces are presented in Figure 33.

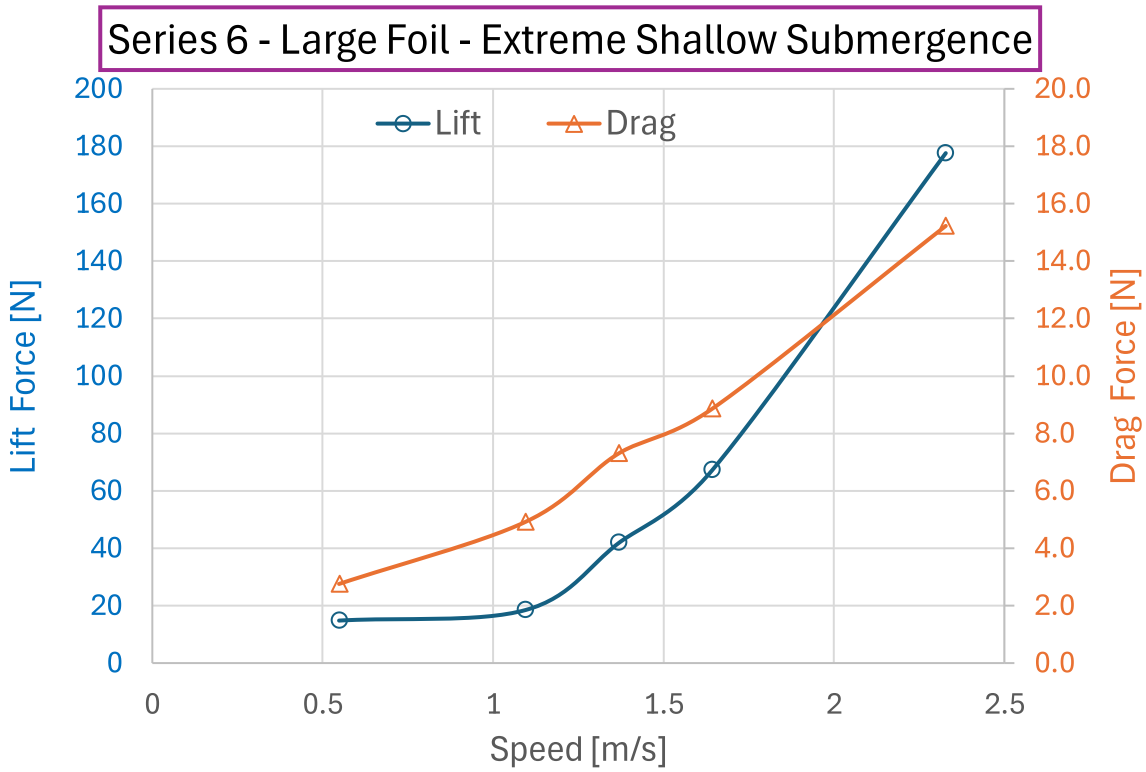

Figure 33- Series 6- Lift and Drag forces measured in calm condition with extreme shallow submergence.

During the very shallow submergence tests, wave breaking was observed at the free surface at low towing speeds (Figure 34). As the speed increased, the wave crest shifted downstream, and a more stable and repeatable free-surface wave pattern developed at higher speeds.

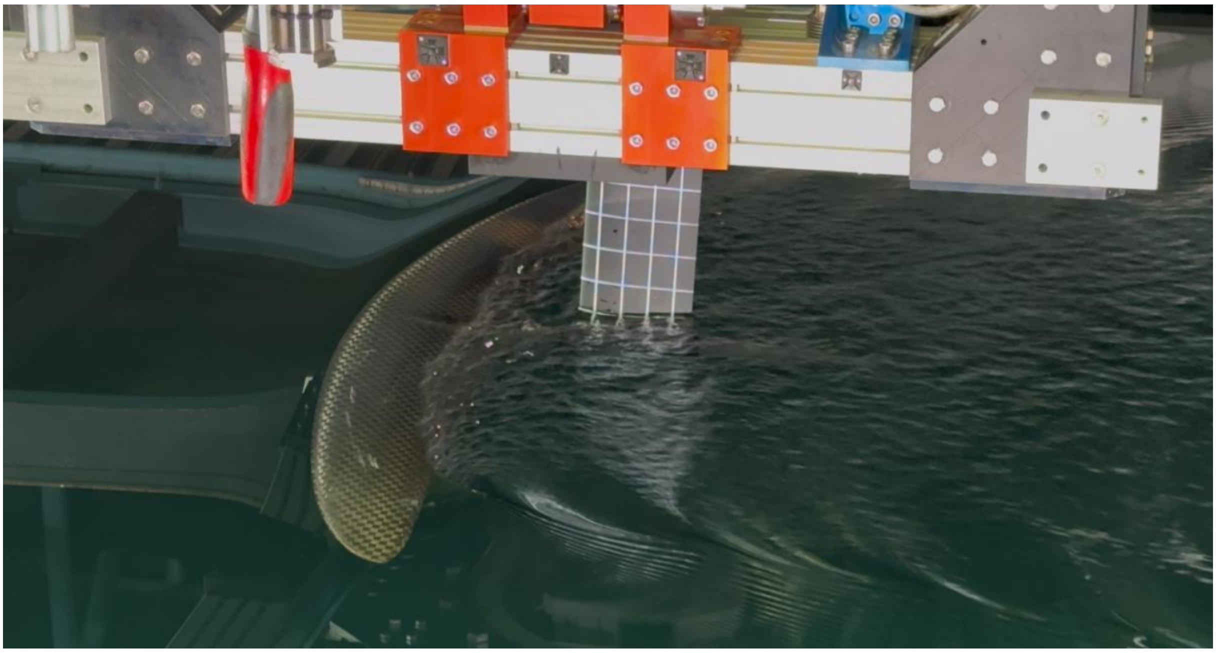

Figure 34- Extreme shallow submergence test series 6 at low speed (0.55 m/s).

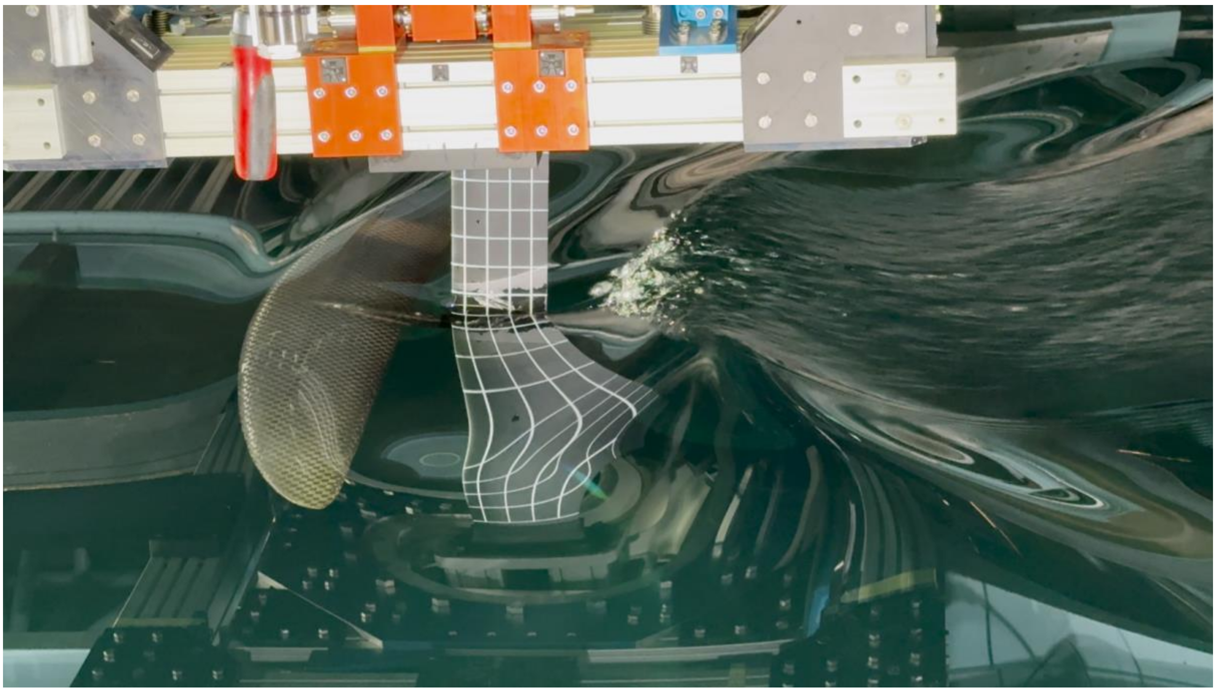

Figure 35- Extreme shallow submergence test series 6 at low speed (1 m/s).

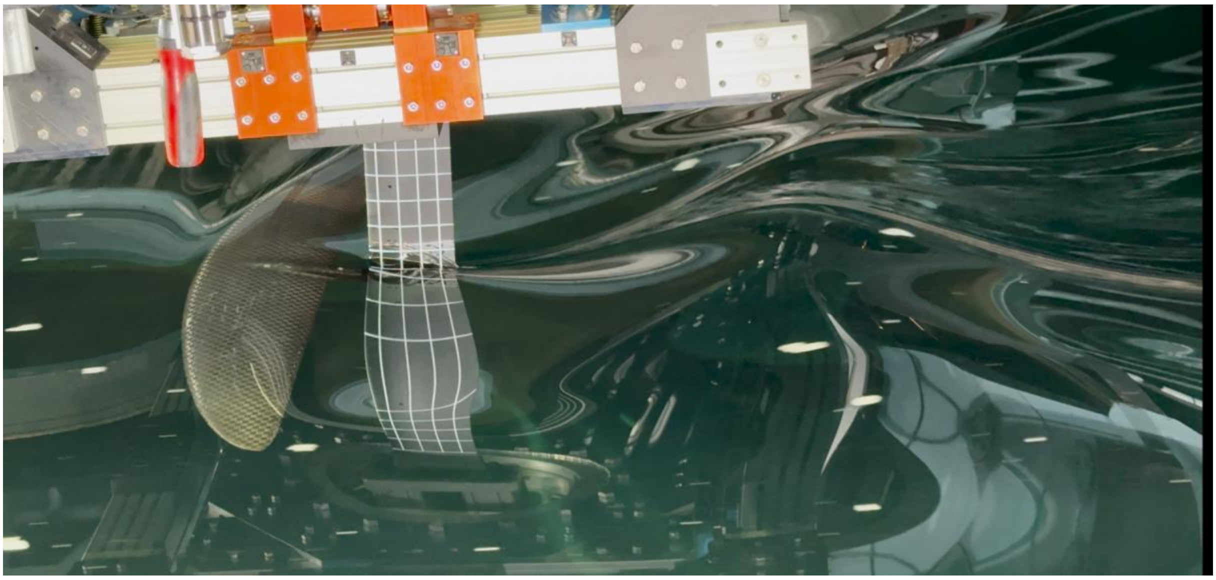

Figure 36- Extreme shallow submergence test series 6 at higher speed (1.5 m/s).

4.8 Series 7 – Calm Water – Large Foil - Submergence 80 mm – AoA 0°

This calm water test series used the **large hydrofoil.** The **lift and drag forces** acting on the complete foil system, comprising the **wing (foil), fuselage, and mast,** were measured. The corresponding **test conditions** and **foil specifications** are summarized in Figure 37.

Test condition		
Depth	80	mm
H/C	0.42	
AoA	0	deg
Wave condition	calm	
Wavelength	0	m
Wave height	0	mm

Large Foil - gong-galaxy, Wing Curve H v2, 3XL		
Chord Length	191	mm
Wingspan	1250	mm
Wingspan²/surface area ratio	8.4	
Thickness	24	mm
Volume	2.43	lit
Projected area	1850	cm²
Extrados area	1918	cm²
Felt area	1850	cm²

Figure 37 - Test Series 7 – tables of specifications.

Tests were conducted at an extreme shallow submergence 80 mm, while the towing speed was varied up to 2.3 m/s. The measured lift and drag forces are presented in Figure 38. This test series was performed to compare the small effect of submergence depth on the lift force while foil is very close to free surface.

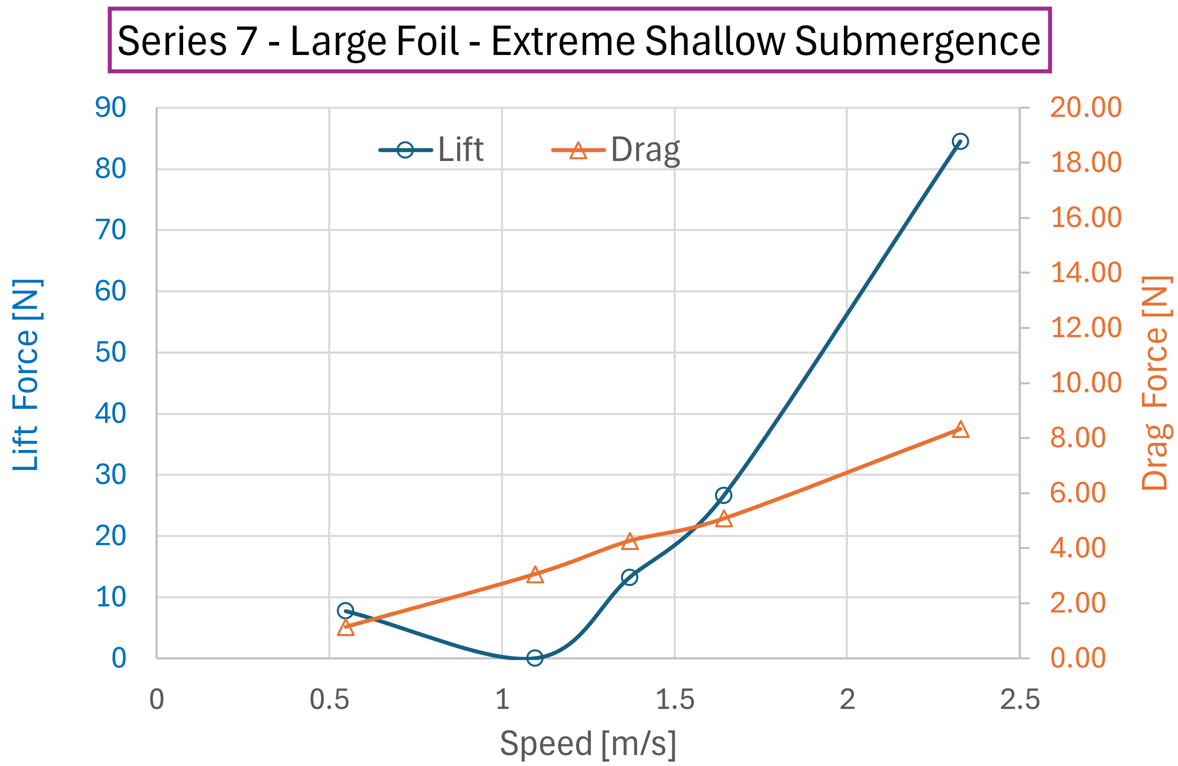

Figure 38- Series 7- Lift and Drag forces measured in calm condition with extreme shallow submergence.

4.9 Series 5 – Regular Following Waves – Submergence 400mm

This test series used the **large hydrofoil** in following wave configuration. The foil is mounted backward, and the measurement was performed while the carriage moved in the direction of wave propagation from end of the basin (Figure 39).

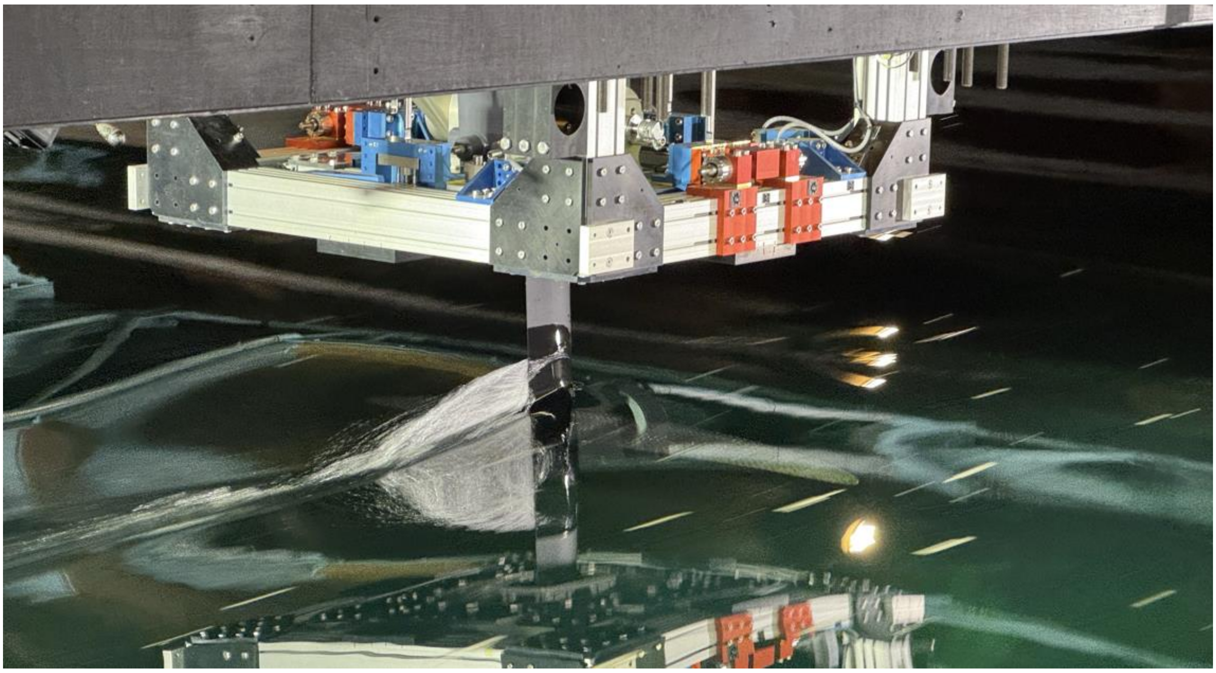

Figure 39- Series 5 foil mounting configuration.

The **lift and drag forces** acting on the complete foil system, comprising the **wing (foil), fuselage, and mast,** were measured. The corresponding **test conditions** and **foil specifications** are summarized in Figure 40.

Test condition		
Depth	400	mm
H/C	2	
AoA	4	deg
Wave condition	Following	wave

Large Foil - gong-galaxy, Wing Curve H v2, 3XL		
Chord Length	191	mm
Wingspan	1250	mm
Wingspan²/surface area ratio	8.4	
Thickness	24	mm
Volume	2.43	lit
Projected area	1850	cm²
Extrados area	1918	cm²
Felt area	1850	cm²

Figure 40- Test Series 5 – tables of specifications.

Regular waves with different wavelengths and amplitude are generated at the end of basin (Figure 41).

Figure 41- Regular waves generated with the wavemakers located at the end of basin.

Table 2 - Regular wave condition in the following wave test series 5.

Regular Wave Condition					
Run No.	Amplitude H [m]	Wavelength λ [m]	Wave Period T [s]	Phase Speed C [m/s]	Foil Speed U [m/s]
3	0.076	5.636	5.636	1	4
4	0.114	5.636	4.5088	1.25	4
6	0.1	4	1.601	1.25	4
7	0.1	3	1.386	1.082	4
8	0.1	2	1.132	0.884	4
9	0.1	1.6	1.012	0.79	4
10	0.06	1.6	1.012	0.79	4
11	0.06	2	1.132	0.884	4
12	0.06	3	1.386	1.082	4
13	0.06	4	1.601	1.25	4
14	0.06	2	1.132	0.884	2.83
15	0.06	3	1.386	1.082	3.46

As the Table 2 shows, the following wave test was conducted in two stages. First, the foil was towed at a constant speed of 4 m/s while the wave amplitude and wave phase speed were varied across a range of combinations. Subsequently, selected runs were repeated at different foil speeds while keeping the wave amplitude constant. Because these measurements were performed in waves, the instantaneous lift and drag forces were recorded together with the local free surface elevation at the two measurement locations described previously (Figure 42).

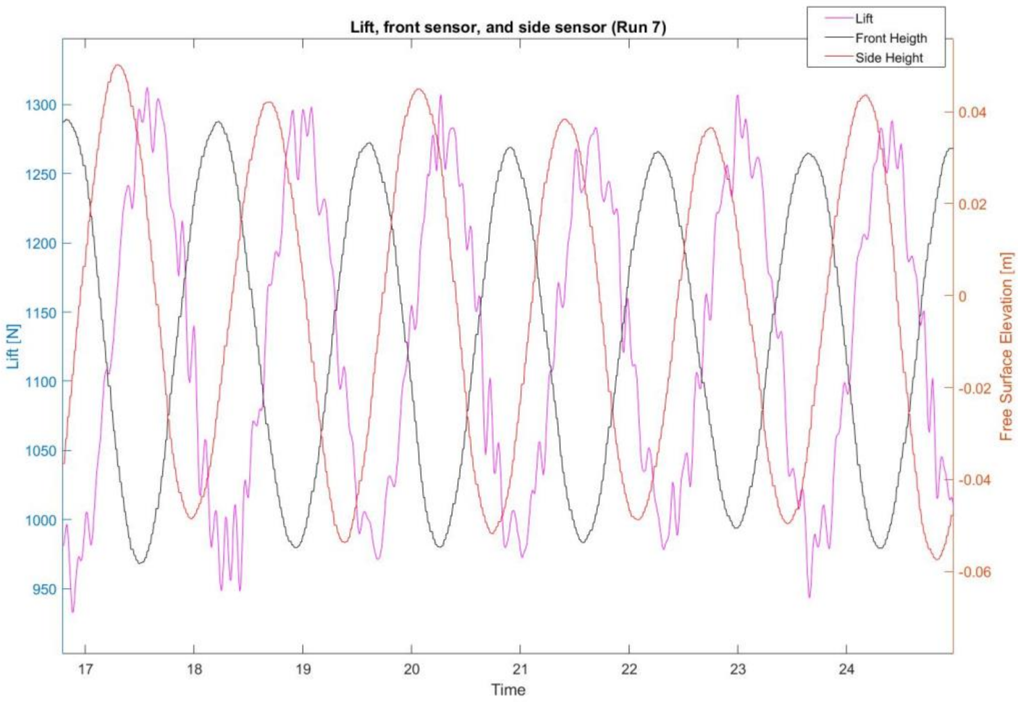

Figure 42 – An example of the lift force and elevation measurement in two locations following the wave in series 5.

4.10 Series 8 – Regular Head Waves – Large Foil – Submergence 400mm

This test series used the **large hydrofoil** in head wave configuration. The foil is mounted similar to the calm water condition and the carriage moved in opposite the direction of wave propagation from end of the basin. The **lift and drag forces** acting on the complete foil system, comprising the **wing (foil), fuselage, and mast,** were measured. The corresponding **test conditions** and **foil specifications** are summarized in (Figure 43).

Test condition		
Depth	400	mm
H/C	2	
AoA	4	deg
Wave condition	Head wave	

Large Foil - gong-galaxy, Wing Curve H v2, 3XL		
Chord Length	191	mm
Wingspan	1250	mm
Wingspan²/surface area ratio	8.4	
Thickness	24	mm
Volume	2.43	lit
Projected area	1850	cm²
Extrados area	1918	cm²
Felt area	1850	cm²

Figure 43- Test Series 8 – tables of specifications.

Regular waves with different wavelengths and amplitude are generated by the wave maker at the end of the basin. As the Table 3 shows, the head wave test was conducted in with constant speed of 4 m/s and constant amplitude while the wave phase speed was varied.

Table 3 - Regular wave condition in the head wave test series 8.

Regular Wave Condition					
Run No.	Amplitude H [m]	Wavelength λ [m]	Wave Period T [s]	Phase Speed C [m/s]	Foil Speed Vs [m/s]
3	0	0	0	0.000	4
4	0.06	1.6	1.012	0.791	4
5	0.06	2	1.132	0.883	4
6	0.06	3	1.386	1.082	4
7	0.06	4	1.601	1.249	4

Because these measurements were performed in waves, the instantaneous lift and drag forces were recorded together with the local free surface elevation at the two measurement locations described previously (Figure 44Figure 44- An example of the lift force and elevation measurement in two locations following the wave in series 8.).

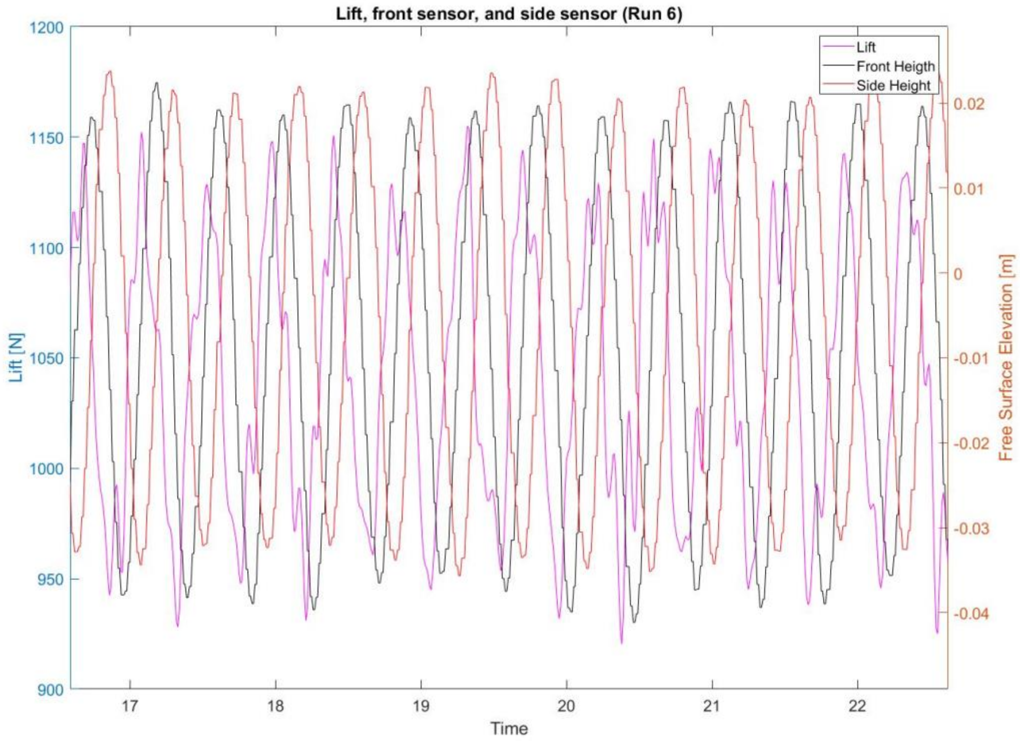

Figure 44- An example of the lift force and elevation measurement in two locations following the wave in series 8.

A series of stationary wave elevation measurements was also conducted to calibrate the wave amplitude and wavelength for each prescribed wave condition.

5 Highlighted Findings and Summary

In this work, a dedicated test rig for hydrofoil force measurements was designed and manufactured, and an experimental campaign comprising 8 test series was completed under both calm water and wave conditions. The calm water tests included a foil scale comparison and an investigation of lift sensitivity to submergence, with particular emphasis on near surface operation. These measurements were intended to quantify the influence of submergence when the foil is positioned close to the free surface. The lift force increased with increasing submergence for $H/C > 1$.

Although the selected foil family is well suited for scale comparison studies, the present mounting arrangement introduces an additional source of uncertainty when operating at non-zero angle of attack. Specifically, pitching the mast/foil assembly changes the effective submergence, and the resulting sensitivity of submergence to alignment and adjustment limits the accuracy of depth control. For repeated measurements with the same foil system, it is therefore recommended to conduct baseline tests at zero angle of attack, thereby reducing uncertainty associated with the submergence determination.

The current rig enables testing at fixed submergence under controlled towing conditions. Future iterations could be enhanced by incorporating dynamic height adjustment and spring-loaded vertical support, to better represent realistic foiling operation. Such modifications would allow the foil to provide an equilibrium elevation under approximately constant lift force (weight of the boat) and would facilitate investigations of unsteady foil dynamics, particularly in waves.

Within the scope of this project, a Master's thesis was conducted by students at Chalmers University of Technology [4]. The thesis focused on the scaling effects in hydrofoil testing and employed Computational Fluid Dynamics (CFD) simulations to investigate the influence of model scale on hydrofoil performance. The thesis project aimed to assess various scaling effects on a horizontal hydrofoil and to develop a feasible methodology for evaluating foil performance in a towing tank. The limitations of the towing tank were identified, and flow effects related to submergence depth and testing velocity were examined using the CFD software STAR-CCM+. Parametric studies on submergence depth and velocity were conducted using the generic hydrofoil profile Eppler 818. The results indicate that wave characteristics significantly influence lift generation, and the findings subsequently contributed to the design of the test rig.

Aston Harald, representing the industrial partners in this project, manufactured a carbon-fibre composite hydrofoiling model boat. The hull was originally developed as electric foiling boat for the Swedish Sea Rescue Society in ELLIN and NG-FREEBS project, the in-kind contributions to this project. The 1.8 m model is currently used at RISE/SSPA as a research platform for a range of projects, including hydrofoil testing and autonomous manoeuvring.

Figure 45 - SSRS06 foiling model boat designed for Swedish Sea Rescue Society and manufactured by Aston Harald.

6 References

[1] R. Vellinga, Hydrofoils: Design, Build, Fly, Peacock Hill Publishing, 2009.

[2] L. Marimon Giovannetti, A. Farousi, F. Ebbesson, A. Thollot, A. Shiri, A. Eslamdoost, Fluid-structure interaction of a foiling craft, Journal of Marine Science and Engineering 10 (2022) 372.

[3] N. Lundqvist, E.L. Favrum, Hydrodynamic Design, System Design and Control System for a Model-Scale Foiling Boat, Master Thesis, Chalmers, 2022.

[4] M. Varvne, W. Eriksson, Scaling Effects for Hydrofoils Testing, Master Thesis, Chalmers, 2024.

[5] O.M. Faltinsen, Hydrodynamics of High-Speed Marine Vehicles, Cambridge Univ. Press, 2007.

[6] R. Andersson, S. Granli, Free Surface Effects on Horizontal Hydrofoils, Master Thesis, Chalmers, 2018.